Development of inversion methods on fault slip data: Stress state in orogenes of the Central Asia

Article *in* Tectonophysics · December 2012
DOI: 10.1016/j.tecto.2012.09.027

CITATIONS
32

READS
165

4 authors, including:

Yu. L. Rebetsky
Russian Academy of Sciences
179 PUBLICATIONS **379** CITATIONS
SEE PROFILE

Nailia Sycheva
Research station of RAS
23 PUBLICATIONS **107** CITATIONS
SEE PROFILE

R. E. Tatevossian
Russian Academy of Sciences
65 PUBLICATIONS **739** CITATIONS
SEE PROFILE

Tectonophysics xxx (2012) xxx–xxx

Contents lists available at SciVerse ScienceDirect

Tectonophysics

journal homepage: www.elsevier.com/locate/tecto

Development of inversion methods on fault slip data Stress state in orogenes of the Central Asia

Yu.L. Rebetsky [a,*], O.A. Kuchai [b,1], N.A. Sycheva [c,2], R.E. Tatevossian [a,3]

[a] Institute of the Physics of Earth, Russian Academy of Sciences (RAS), Moscow, Russia
[b] Institute of Oil Geology & Geophysics, Siberian Div., RAS, Novosibirsk, Russia
[c] "Bishkek" Research Station under RAS, Bishkek, Kyrgyzstan

ARTICLE INFO

Article history:
Received 8 January 2011
Received in revised form 14 August 2012
Accepted 28 September 2012
Available online xxxx

Keywords:
Earthquakes
Focal mechanisms
Inversion problem of tectonophysics
Slip fault data
Stresses
Central Asia

ABSTRACT

Algorithm of natural stress reconstruction based on data on slip fault sets is presented. Also additional physical principles following from generalization of experimental geomechanics and theoretical tectonophysics are considered. It gives possibility to define not only orientation of stress tensor principal axis but also the ratio of its spherical and deviatory components. The characteristic feature of the method is that it simultaneously calculates mutually consistent components of stress tensor and increment tensor of seismotectonic deformations, what was missing in previously known methods of tectonophysics. The application of the method is illustrated by two case studies in seismoactive zones of Central Asia: a) Altai and Sayan and b) Northern Tien Shan. Results of stress reconstruction in this intra-plate faulted and folded domains demonstrate that the impact of crust flow and mantle heterogeneity on stresses is great. These processes can contribute much more in generating stresses in crust than interaction of lithosphere plates at distant borders.

1. Introduction

Methods of analysis of seismological data on earthquake source mechanisms and geological information on orientation of slip fault sets are well-known in inverse problem of tectonophysics. These methods of stress inverse problem make it possible to calculate four out six components of tectonic stress tensor based on data on discontinuous dislocation: orientation of three principal stress axis (σ_k, $k=1,2,3$), determined by three Euler's angles and Lode–Nadai or ratio coefficient characterizing shape of stress tensor.

In Europe, methods of reconstructing regional stresses based on geological field data on the fault slip sets have actively started thanks to activities of French school (Angelier, 1975a,b,c; Armijo and Cisternas, 1978; Arthaud, 1969; Carey and Bruneier, 1974; Mercier et al., 1973). J. Angelier contributed greatly in this research field. Methods developed by J. Angelier, i.e. right quadrants (Angelier and Mechler, 1977), system of conjugate faults (Angelier, 1979; Angelier, 1989a) and analytical averaging (Angelier, 1990), are intensively used by tectonophysicists.

Tectonophysicists and seismologists in Russia, working independently and in parallel, developed methods of reconstruction of stresses and increment of seismotectonic deformations using similar initial data type and basic postulates (Danilovich, 1961; Gushchenko, 1975; Gushchenko and Kuznetsov, 1979; Gushchenko and Sim, 1974; Nikitin and Yunga, 1977; Parfyonov, 1981; Riznichenko, 1965, 1977; Stepanov, 1979; Yunga, 1979). O.I. Gushchenko led this scientific school in Russia. He developed several versions of procedure for the method of kinematic analysis of faults. J. Angelier and O.I. Gushchenko contributed definitely in the development of tectonophysic methods of natural stress reconstruction. At a certain stage they met and collaborated (Angelier, et al., 1994), and tragically, too early left us.

The above mentioned methods should be considered as further development of methods of tectonic stress analysis based on data on conjugate pair of slip faults formulated by E. Anderson (1951) and M.V. Gzovsky (1954, 1956), which make it possible to determine only orientation of principal stresses. It has to be marked that there is a principal difference between approaches by Anderson–Gzovskiy and Angelier–Gushchenko. The first approach was completely based on results of rock failure mechanics and assumed isotropy of properties of geological media; the second one is based on postulates of dislocation plasticity, assuming presence of strength defects in geological objects. Further on, this approach was developed by large group of researchers (Reches, 1978, 1983, 1987; Lisle, 1979, 1987, 1992; Etchecopar et al., 1981; Gintov and Isai, 1984a,b; Michael, 1984; Gephart and Forsyth, 1984; Aleksandrowski, 1985; Bergerat, 1987; Rivera and Cirsternas,

* Corresponding author at: 123995, B. Gruzinskaya, 10, IPE RAS, Moscow, Russia. Tel.: +7 9031739602.
E-mail addresses: reb@ifz.ru (Yu.L. Rebetsky), KuchayOA@ipgg.nsc.ru (O.A. Kuchai), nelya@gdirc.ru (N.A. Sycheva), ruben@ifz.ru (R.E. Tatevossian).
[1] Prospect Academika Koptuga, 3, Novosibirsk, 630090, Russia.
[2] Research Station under RAS, 720049, Bishkek-49, Kyrgystan.
[3] B. Gruzinskaya, 10, IPE RAS, 123995, Russia, Moscow.

0040-1951/$ – see front matter © 2012 Elsevier B.V. All rights reserved.
http://dx.doi.org/10.1016/j.tecto.2012.09.027

1990; Yunga, 1990; Mostrjukov and Petrov, 1994; Rebetsky, 1996; Yamaji, 2000; etc.).

In this paper method of cataclastic analysis of geological data on slip faults or seismological data on earthquake source mechanisms (MCA) is presented. It is developed in Russia since the 1990s (Rebetsky, 1996, 1997, 1998a,b, 1999; Rebetsky and Fursova, 1997) as continuation of brilliant works by J. Angelier. At the beginning the method was designed only to assess relative values of spherical and deviatory stress components (Rebetsky, 2003, 2005a). Later on it was upgraded to determine components of complete stress tensor and parameters of effective strength of rocks (Rebetsky, 2007, 2009a,b,c; Rebetsky and Marinin, 2006a,b). To illustrate the MCA power we will present results of reconstruction of stresses in earth crust of large intra-plate fold and thrust belt in Central Asia: Northern Tien Shan and Altai and Sayan.

2. The cataclastic analysis method

The MCA consists from sequence of four reconstruction stages. One or several components of stress tensor and parameters of effective strength of rock massive is determined at each stage. At the first stage fundamental principles of plasticity are used to determine parameters of the stress ellipsoid. At the second stage, generalized relationships of experimental geomechanics are used to determine relative components of effective confining stress and maximal shear stresses. At the third and forth stages, additional seismological and geophysical constraints are used to define absolute values of stresses. At each following stage, parameters of the stress components obtained at previous stage are used. In this paper will be presented algorithms related only to the first and second stages of the MCA. Correspondingly, only results of these stages will be analyzed for orogene zones in Central Asia.

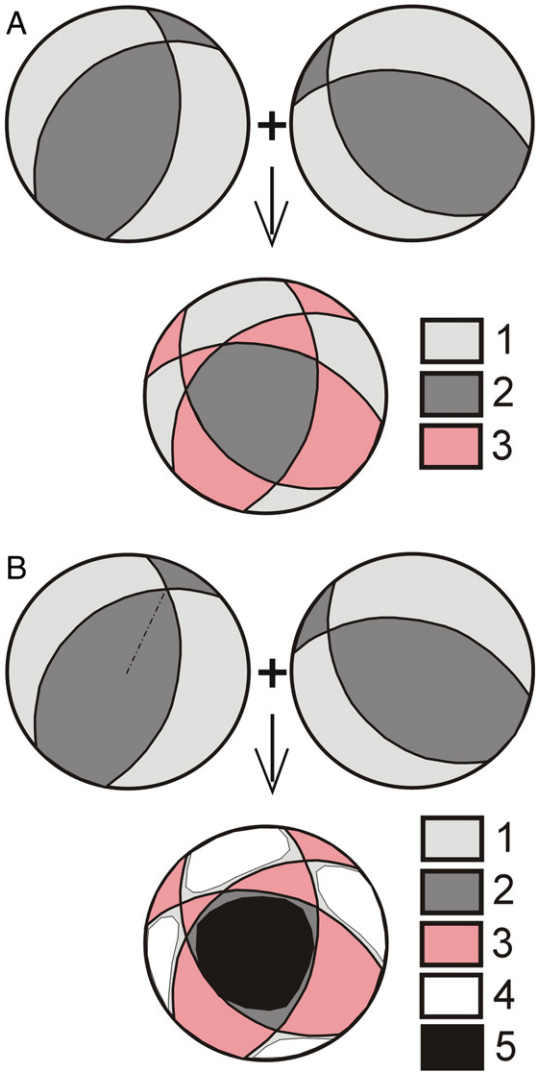

Fig. 1. The scheme of summation procedure of areas of permissible and unpermissible orientation of principal stress axes on lower unit hemisphere for two earthquake focal mechanisms: (A) — on the basis of inequalities (Eq. (6)); (B) — on the basis of inequalities (Eq. (5)). 1, 2 — areas of permissible orientation of axes σ_1 and σ_3 respectively per one earthquake mechanism; 3 — areas of unpermissible orientation for axes σ_1 and σ_3 on two mechanisms on the basis of inequalities (Eq. (6)); 4, 5 — areas of permissible orientation for axes σ_1 and σ_3 respectively on two mechanisms on the basis of inequalities (Eq. (5)).

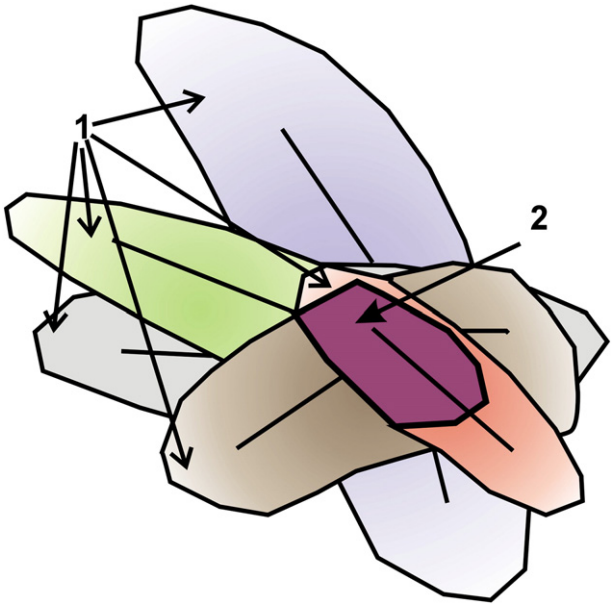

Fig. 2. Zone of cumulative crossing of areas of the elastic unloading formed around of faults. Grid node if stress reconstruction should be within of this cumulative area. 1 — Individual areas of elastic unloading of earthquakes and 2 — cumulative area of elastic unloading of many earthquakes. Thick black lines — faults (earthquake sources).

2.1. Algorithm of the first stage of MCA

First of all homogeneous samples of slip faults have to be compiled. Samples represent homogeneous in space and time stage of earth crust deformation process.

Such demand is characteristic also in methods by J. Angelier and O.I. Gushchenko. They have formulated algorithms of compilation of homogeneous samples of slip fault sets based on the assumption that slip vectors in the fault plane coincides with the direction of shear stress over it (Bott, 1959; Wallace, 1951). For seismological data on this assumption means that the quadrants of permissible location of stresses σ_1 and σ_3 of the given earthquake are in accordance with such quadrants of earthquake mechanism (McKenzie, 1969). Postulate that direction of striation coincides with direction of shear stresses on the fault plane is the basis in the dislocation theory of plasticity (Batdorf and Budiansky, 1954).

As it is in J. Angelier and O.I. Gushchenko methods, also in the MCA it is assumed that slip faults, occurred under quasi-homogeneous stress regime, use existing defects of strength in rock massive. However, in the MCA it is not postulated that slip direction coincides with shear stresses acting over future fault plane. It is just enough that the energy of elastic strain decreases as a result of dislocations. The other requirement within the MCA method is that stress tensor defined for the set of dislocations from homogeneous sample has to ensure maximum of elastic energy dissipation.

Please cite this article as: Rebetsky, Yu.L., et al., Development of inversion methods on fault slip data, Tectonophysics (2012), http://dx.doi.org/10.1016/j.tecto.2012.09.027

2.1.1. Criteria for compilation of homogeneous sample

As in other methods, increments of seismotectonic deformations are associated with irreversible deformations along slip fault planes within the fractured rock massive. For calculation of increment tensor of seismotectonic deformations generated by a single fault we will use expression by (Kostrov, 1975; Kostrov and Das, 1988):

$$de_{ij}^{\alpha} = \frac{\Omega^{\alpha} D^{\alpha}}{2V^{\alpha}} \left(\swarrow_{ni}^{\alpha} \swarrow_{sj}^{\alpha} + \swarrow_{nj}^{\alpha} \swarrow_{si}^{\alpha} \right), i,j = 1,2,3. \quad (1)$$

Expression (1) defines impact of shift along the fault with number α in the irreversible deformation tensor averaged for all points within the elastic unloading V^{α}. In Eq. (1) $\swarrow_{ni}^{\alpha}$ and $\swarrow_{si}^{\alpha}$ $(i=1,2,3)$ are direction cosines of unit vector normal to the crack plane n and displacement vector s in any orthogonal coordinate system (i, j, k), D^{α} is mean slip along fault plane, and Ω^{α} is the fault area. Sum of the impacts from individual earthquakes within certain volume represents the tensor of seismotectonic deformations of the volume.

Introducing the concept of the volume of elastic unloading V^{α} is required for calculation of irreversible deformations. Due to this concept it is possible to link residual deformations formed as a result of slip faults to the volume, where elastic deformations decrease (see next section).

In plasticity theory there is accordance condition between components of stress tensor and increment of plastic deformations (Chernykh, 1988):

$$\left(\sigma_i - \sigma_j\right)\left(de_{ii}^{p} - de_{jj}^{p}\right) \geq 0, i,j = 1,2,3 \quad (2)$$

where de_{ii}^{p} is the component of increment of plastic deformations of elongation and shortening in directions of principal stress axis σ_i. From Eq. (2) and according to the condition assumed in geodynamics $\sigma_1 \geq \sigma_2 \geq \sigma_3$ (compression is positive), it follows:

$$de_{11}^{p} \geq de_{22}^{p} \geq de_{33}^{p} \text{ when } de_{11}^{p} + de_{22}^{p} + de_{33}^{p} = 0. \quad (3)$$

According to Eq. (3) irreversible plastic deformations of elongation and shortening in direction of principal axis are defined according to the axis' index. 1) Elongation is along σ_3 ($de_{33}^{p} < 0$). 2) Shortening is along σ_1 axis ($de_{11}^{p} > 0$). 3) Along with σ_2 axis either elongation or shortening (de_{22}^{p}), which modules has to be smaller than deformations along two other principal axis. This impose constrains on the character of the plastic flow for wide range of materials including anisotropic ones. Note that from the condition of incompressibility (second condition in Eq. (3)) it follows a system of inequalities used by J. Angelier and O.I. Gushchenko (Angelier, 1979; Angelier and Mechler, 1977; Gushchenko, 1979; Gushchenko and Kuznetsov, 1979).

After the first stage of the MCA it is possible to define Euler's angles, which describe orientation of principal axis of stress tensor, and the shape of stress ellipsoid based on values of the coefficient μ_{σ}, because components of the stress tensor can be presented as (Nadai and Wahl, 1931):

$$\sigma_{ij} = p\delta_{ij} + \tau\left[\left(1 - \frac{1}{3}\mu_{\sigma}\right) \swarrow_{1i} \swarrow_{1j} + \frac{2}{3}\mu_{\sigma} \swarrow_{2i} \swarrow_{2j} - \left(1 + \frac{1}{3}\mu_{\sigma}\right) \swarrow_{3i} \swarrow_{3j}\right],$$
$$\text{where } p = (\sigma_1 + \sigma_2 + \sigma_3)/3, \tau = |\tau_{\max}| = (\sigma_1 - \sigma_3)/2, \mu_{\sigma} = 1 - 2\Phi. \quad (4)$$

Expression in square brackets characterizes stress ellipsoid (its shape and orientation of principal axis). Therefore, after realization of the first stage of the MCA, confining pressure p and module of maximal shear stress τ are left undefined out of six components of stress tensor. These parameters are the most interesting for tectonophysics and geomechanics. In expression (4) $\swarrow_{ki}$ are directing cosines of principal stresses σ_k, $k=1, 2, 3$ in arbitrary coordinate system, δ_{ij} is Kronecker delta, and Φ is stress ellipsoid shape ratio (Angelier and Mechler, 1977).

We assume that limiting condition (3) is true for each separate act of generating irreversible deformations by individual slip over a fault (hypothesis 1). Accepting as coordinate system orthogonal triad of principal axis and applying Eq. (1) in Eq. (3) one gets the main criterion of the MCA, which determines dissipation of elastic strain of rock massive after activation of each slip fault and regularity in developing irreversible deformations:

$$\swarrow_{n3}^{\alpha} \swarrow_{s3}^{\alpha} \geq \swarrow_{n2}^{\alpha} \swarrow_{s2}^{\alpha} \geq \swarrow_{n1}^{\alpha} \swarrow_{s1}^{\alpha} \text{ when } \swarrow_{n1}^{\alpha} \swarrow_{s1}^{\alpha} + \swarrow_{n2}^{\alpha} \swarrow_{s2}^{\alpha} + \swarrow_{n3}^{\alpha} \swarrow_{s3}^{\alpha} = 0. \quad (5)$$

Here $\swarrow_{gi}$ is the directing cosine of unit vectors n and s ($g=n, s$) in coordinate system of principal stresses σ_k.

These conditions (Eq. (5)) impose stronger constraints on principal stress axis, which we are searching, than those used by J. Angelier (Angelier and Mechler, 1977) and by O.I. Gushchenko (Gushchenko and Kuznetsov, 1979):

$$\swarrow_{n1}^{\alpha} \swarrow_{s1}^{\alpha} \leq 0 \text{ and } \swarrow_{n3}^{\alpha} \swarrow_{s3}^{\alpha} \geq 0. \quad (6)$$

Expressions (6) demonstrate that the principal stress axes σ_1 and σ_3 on unit hemispheres can be located in quadrants of compression or tension correspondingly, plotted in Fig. 1A using vectors of normal n

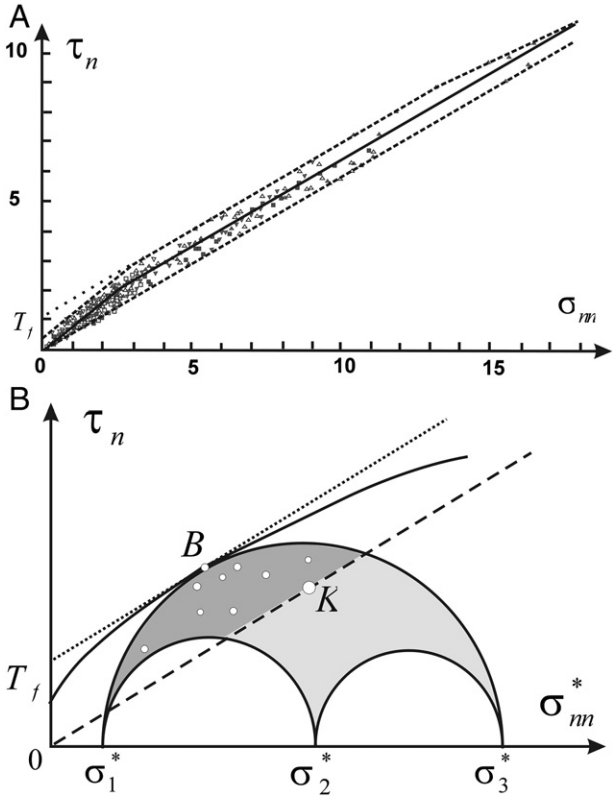

Fig. 3. Zone of brittle failure on Mohr diagram: A) Mohr parametric space τ_n,σ_{nn} (kbar) adapted from Byerlee (1978) with the results of laboratory experiments for strong rock. Solid line is plotted by J. Byerlee across the midst of a cloud of solid circles (stresses on the slip fault planes). Upper dashed line corresponds to the Mohr failure envelope for geo-material (fracture shear strength or Mohr envelope for intact rock (Handin, 1969). Lower dashed line corresponds to the minimum resistance to friction forces (Angelier, 1989b). The range enclosed between two dashed lines means the failure zone or dilatancy zone. B) The simplified form of the zone of brittle failure, used in MCA algorithm. Solid line is the Mohr failure envelope for real geo-material. Upper dotted stright line corresponds to the approximation of the Mohr failure envelope curve. Lower dashed line corresponds to the minimum of static friction stresses. Area of light grey color inside the big and above small circles of Mohr, defines stress states on the planes of different orientation. Area of dark grey color means failure zone for restriction with Eq. (15). Points within the dark gray area are normal and shear stresses on the planes of slip faults from a homogeneous sample. The point K lies on the line of the minimum resistance of friction. σ_i^* and σ_{nn}^* — effective principal and normal stress accordingly.

Please cite this article as: Rebetsky, Yu.L., et al., Development of inversion methods on fault slip data, Tectonophysics (2012), http://dx.doi.org/10.1016/j.tecto.2012.09.027

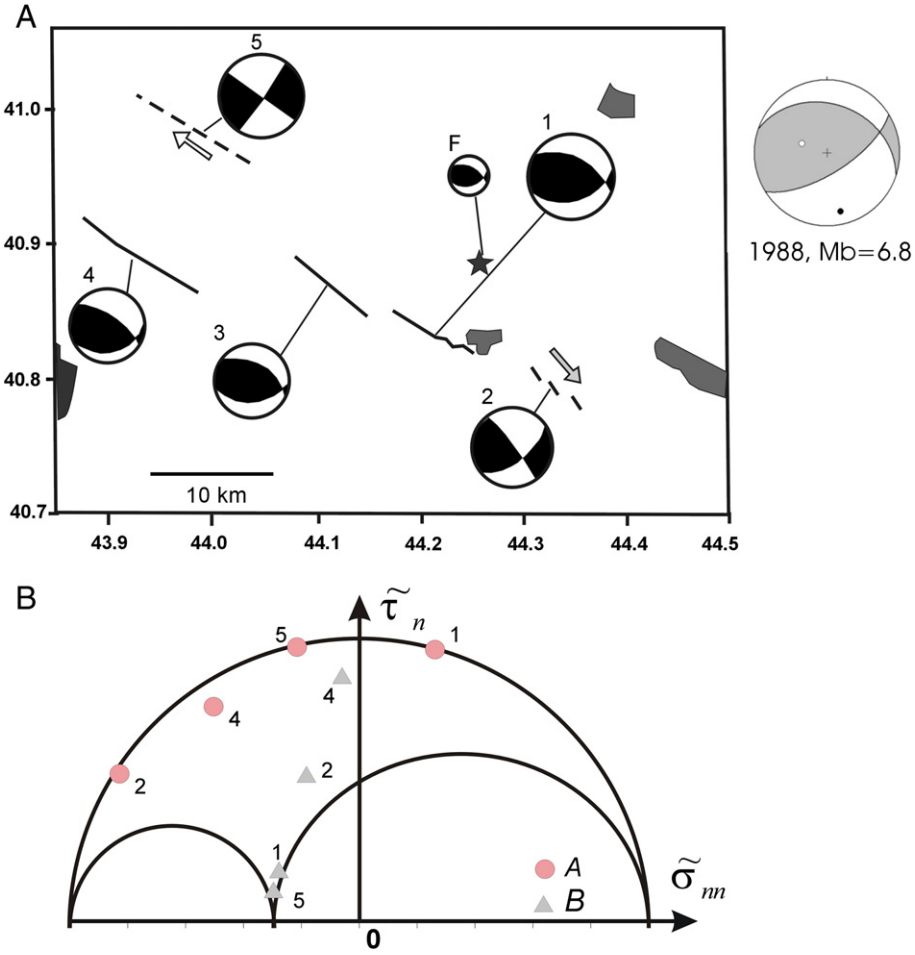

Fig. 4. Mechanisms of the sub-sources of Spitak (Armenia, 1988, $M_b = 6.8$) catastrophic earthquake (A) and the analysis of the acting stresses on its nodal planes by the reduced Mohr diagram (B). Small circles (A) mean the realized nodal planes (faults) which have passed check of criterion (20). Small triangles (B) mean the second nodal planes each earthquake focal mechanisms. F and 3 coincide with number 1.
Panel a is from Arefiev et al. (2005).

and displacement *s*. J. Angelier and O.I. Gushchenko make a sum of opposite quadrants — ones, which are forbidden for the corresponding principal stress axis. By this they found areas over unit hemispheres on σ_1 and σ_3.principal axes. Such approach leads to progressively narrowing convolution of areas of permissible orientation of the principal axis.

System of inequalities (Eq. (5)) used in the MCA makes it possible for the same amount of events in the homogeneous sample of slip faults to localize areas of principal stresses on unit hemisphere much faster (Fig. 1B). The economy due to the additional inequality becomes visible after summing of two earthquake mechanisms.

The set of events satisfying conditions (5) is called *homogeneous sample of earthquake sources*, which characterizes quasi-homogeneous deformation of certain crust domain in the vicinity of grid node for stress calculation.

2.1.2. Cumulative principle of forming of initial sample

In the MCA inequalities (Eq. (5)) play a key role in the formation of homogeneous sample, which is either geological data on slip faults or seismological data on earthquake mechanisms. Selection of events into the homogeneous sample is made from sample, which is compiled based on spatial vicinity criterion. This is the initial sample.

For geological data on slip faults, all data collected from the same geological outcrop is taken into the initial sample. It is assumed that these fractures are closely located and are formed under more or less homogeneous loading.

When analyzing stresses based on seismological data it is also required to generate earthquake sample, which characterizes homogeneous stress-state of certain crust domain. To achieve this, the condition of elastic unloading is used. The criterion to include the given dislocation in the initial sample is falling on the grid node of stress reconstruction into the cumulative area of elastic unloading areas (see Fig. 2). The R^α radius of elastic unloading for each earthquake is calculated using data on earthquake source length L^α using formula:

$$R^\alpha = A + BL^\alpha/2 \text{ while } L^\alpha = 10^{(a+bM_b^a)}\,\text{km} \qquad (7)$$

where A characterizes the accuracy of hypocenter location, B is the coefficient determining relationship between fault length L^α and area of its impact on the surrounding volume. According to Wells and Coppersmith (1994) coefficients a and b for strike–slip type earthquakes are −3.55 and 0.74; for reverse fault type −2.86 and 0.63; and for normal fault type −2.01 and 0.50.

In the mechanics of brittle fracture it is demonstrated that the impact of the activated slip fault on the stress-state of the nearby volume is approximately 2–3 times with that of the crack length L (Osokina, 1987). In this area the variation of stress is 2–3% from the mean close to the crack. Such relationship is determined by the fact that decreasing of disturbance in stress is proportional to $1/L^2$. Therefore, for coefficient B values 6–8 can be assumed as first (standard) approximation for calculating the radius R^α of unloading domains of individual earthquake. From the other hand from problem of plasticity theory it is known

Please cite this article as: Rebetsky, Yu.L., et al., Development of inversion methods on fault slip data, Tectonophysics (2012), http://dx.doi.org/10.1016/j.tecto.2012.09.027

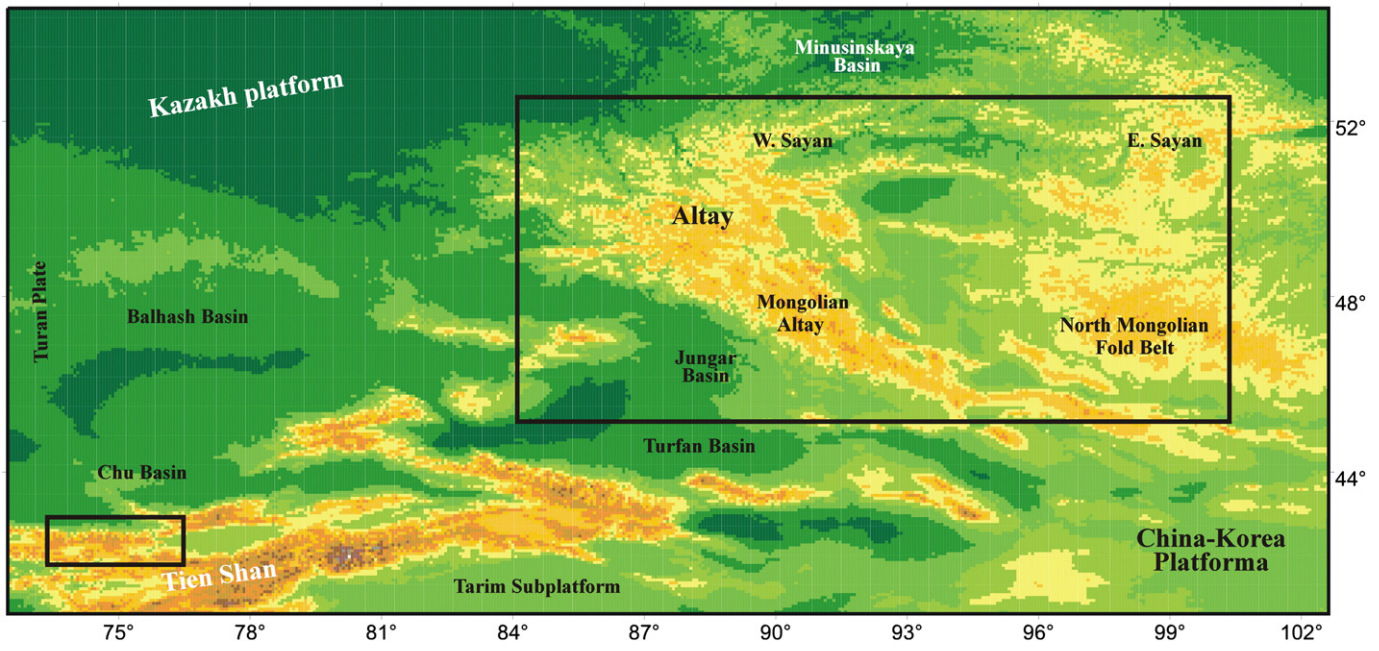

Fig. 5. Map of the Central Asian fold and thrust belt and sedimentary basins. Areas of tectonophysical analysis of the modern stress state are allocated by two rectangles of differing size.

that disturbances in media located in plastic deformation zone in diagram of loading decreases proportional to $1/L$. It means that in such volumes coefficient can increase up to 30 or even 100. Selection of coefficient B strongly depends on earthquake distribution density and accuracy of generating homogeneous sample according to (5), when the coefficient has to be increased with respect to standard values. In the MCA for earthquakes within magnitude range 4.5–6 (M_b), normally, coefficient B varies from 10 to 30.

Note, that coefficients in Eq. (7) for L^α are determined for earthquakes with $M_b > 4.8$ (Wells and Coppersmith, 1994). For smaller earthquakes the relationship has to be modified.

The earthquake in the initial sample which does not fit the homogeneity criteria is excluded from the homogeneous sample (see Fig. 1). The result is *homogeneous sample of earthquake source mechanisms*.

2.1.3. Tensor of increment of seismotectonic deformations and principle of maximum in the MCA

Expression (1) characterizes the contribution of each slip fault into the tensor of irreversible deformations. The sum of individual contributions for the set of earthquakes makes it possible to calculate the increment of seismotectonic deformations (Kostrov and Das, 1988):

$$dS_{ij} \approx 0.5 \sum_{\alpha=1}^{A} de_{ij}^{\alpha}. \tag{8}$$

In the MCA, summing is allowed only for events, which satisfy the following two criteria:

1) they have to be included in the initial sample for the given grid node of reconstruction. It means that stress reconstruction node is within the cumulative area of elastic unloading of the given earthquake (see Fig. 2 and expression (7));
2) earthquake source mechanism fits criterion (5). It means that the quadrants of permissible location of stresses σ_1 and σ_3 of the given earthquake are in accordance with such quadrants of other earthquakes from homogeneous sample (see Fig. 1).

Note that in orthogonal coordinate system related to n (normal to crack), s (displacement vector) and m ($i = n, j = s$), non-zero value will have only directing cosines with repeated indexes ($\angle_{nn}^{\alpha} = \angle_{ss}^{\alpha} = 1$). Therefore, expression (1) in such coordinate system can be written in the following form:

$$de_{ns}^{\alpha} \approx 0.5 d\gamma^{\alpha} \text{ when } d\gamma^{\alpha} = \frac{\Omega^{\alpha} D^{\alpha}}{V^{\alpha}} \approx \frac{D^{\alpha}}{L^{\alpha}} \text{ and } de_{ij}^{a} = 0, i, j = n, s, m, ij \neq ns, \tag{9}$$

i.e. all components of deformation increment tensor (Eq. (1)) are zero except de_{ns}^{α}. It represents half of the increment of maximal shear deformation $d\gamma^{\alpha}$ for de_{ij}^{α} tensor (L^{α} characteristic size of fault, earthquake source). Expression (9) is approximate because the earthquake source and its elastic unloading area are not isometric.

Using Eq. (1) and (9), we re-write expression for increment tensor of seismotectonic deformation in the following form:

$$dS_{ij} \approx 0.5 \sum_{\alpha=1}^{A} d\gamma^{\alpha} \left(\angle_{ni}^{\alpha} \angle_{sj}^{\alpha} + \angle_{nj}^{\alpha} \angle_{si}^{\alpha} \right). \tag{10}$$

Expression (10) for increment tensor of seismotectonic deformation is different from the ones in previous works (Brune, 1968; Kostrov and Das, 1988; Nikitin and Yunga, 1977; Riznichenko, 1965), where the volume for normalization was assumed to be constant ($V^{\alpha} = V$) independent from magnitude and was taken out from summation symbol. Taking into account dependence of V^{α} on earthquake source size, when calculating increment tensor of seismotectonic deformation, is important difference between the MCA and previous ones.

In the MCA it is assumed that $d\gamma^{\alpha} \approx d\gamma = const$ (hypothesis 2). It can be confirmed by the relationship between shear deformation and stress-drop within certain assumptions on strength.

2.1.4. Principle of maximum in the MCA

In the MCA, areas of permissible orientation of stress principal axis on unit hemispheres based on Eq. (5), have finite area (see Fig. 1B) and require single location of principal stress axis. In the method by O.I. Gushchenko the single location of principal stress axis is taken as the center of their possible orientations.

In the MCA the single orientation of principal axis within the localized areas of their possible emergence on hemisphere is determined

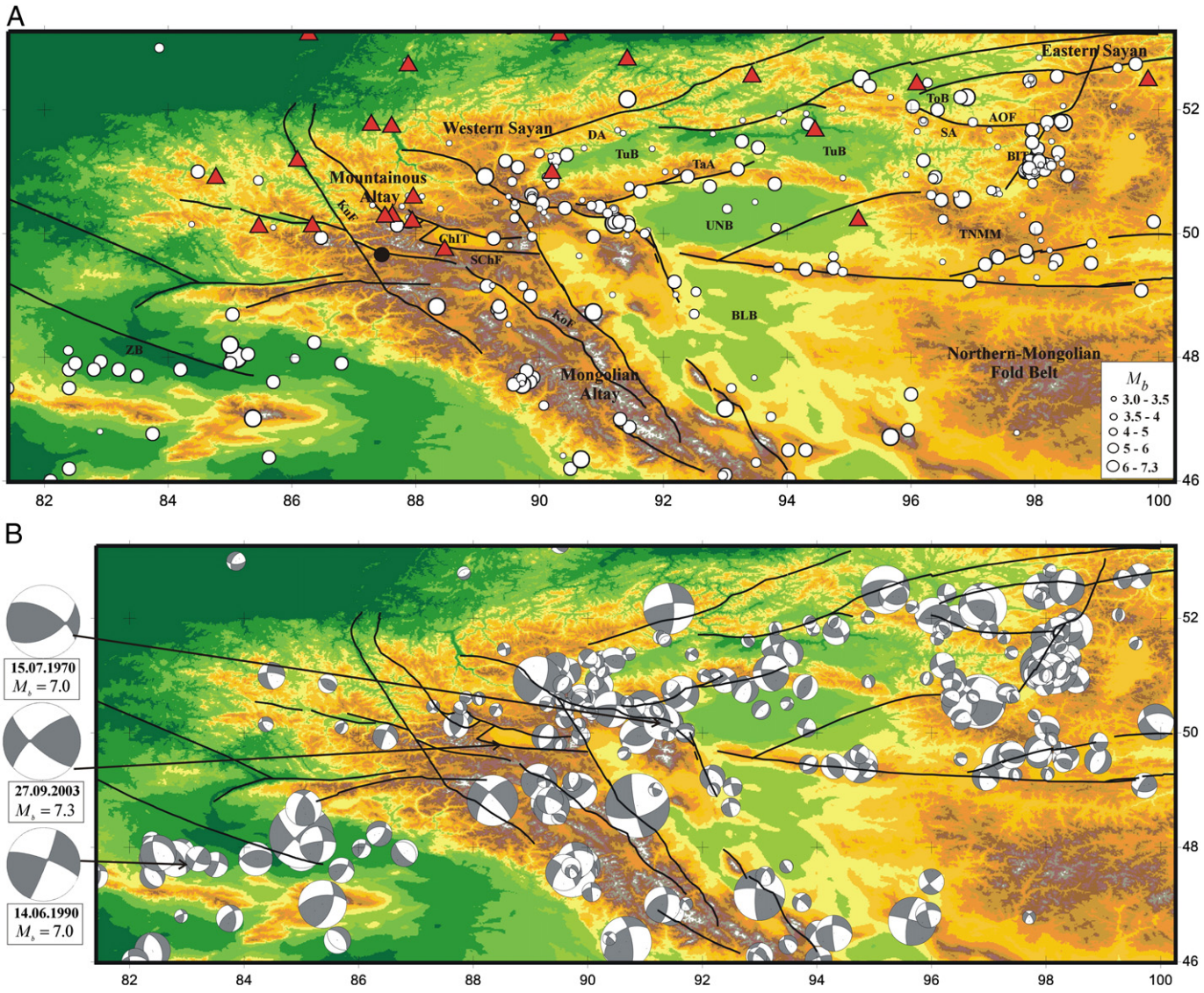

Fig. 6. Tectonic province of Altai and Sayan orogens. Active faults (black lines) by V.V. Trifonov et al. (2002). (A) Distribution of earthquake epicenters from catalogue of earthquake source mechanisms (open circles). Triangles mark the seismic station. Active faults (black lines) by V.V. Trifonov et al. (2002). (B) Earthquake focal mechanism of Altai–Sayan orogen with the range $7 \geq M_b \geq 3$. Earthquakes with $M_b > 7.0$ are taken out for boundary map. Basins, synclinoriums and intermontane troughs: BLB — Big Lakes; ToB — Todjin; TuB — Tuva; UNB — Ubsu–Nur; ZB — Zaisan; BIT — Busingol; and ChIT — Chuya. Anticlinoriums, mountain massifs, blocks and ranges: DA — Djebash; SA — Sangilen; TaA — Tannuol; and TNMM — Tuva–North-Mongolian Range. Faults: AOF — Academician Obruchev; KoF — Kobdo Fault; KuF — Kurai; and SChF — Southern Chuya.

by Mises' principle of maximum, which is the basis of modern theories of plasticity (Drucker, 1949; Hill, 1950)

$$\left(\sigma_{ij} - \sigma'_{ij}\right) de^p_{ij} \geq 0. \tag{11}$$

In Eq. (11) σ_{ij} is the real or searched value of stress components corresponding to the given increment of plastic deformations de^p_{ij}, and σ'_{ij} is the component of any possible stress-state within loading surface, which can be built in six-dimensional space of stress tensor components (Hill, 1950). Expression (11) states that among all possible stress-states the real is the one, for which internal elastic energy dissipation is maximal for the given tensor of plastic deformations.

We assume that de^p_{ij} is equal to the tensor of seismotectonic deformation increment dS_{ij}, which is generated by shift along faults from homogeneous samples (hypothesis 3). We also will consider σ'_{ij} as possible stress tensor with principle axis σ'_1 and σ'_3, falling into domain of their possible orientation (Fig. 1B). Based on Eq. (11), we will define parameters of normalized stress ellipsoid as maximum of function:

$$MAX_{\sigma_{ij}}(F) \text{ when } F = \sigma'_{ij} dS \; for \quad dS_{ii} = 0. \tag{12}$$

F is the function representing the work spent on generating irreversible deformations.

Using Eqs. (4) and (10), hypothesis 2 and uncompression principle of plastic strain (second in Eq. (3)), invariance of tensor product together with standard transformations of stress in different coordinate systems the Eq. (12) can be re-written:

$$\begin{aligned} F &= dS_{ij}\sigma_{ij} = \sum_{\alpha=1}^{A} de^{\alpha}_{ns}\sigma^{\alpha}_{ns} = \tau \; d\gamma \sum_{\alpha=1}^{A} \bar{\sigma}^{\alpha}_{ns} \text{ where } \overline{\sigma}^{\sigma}_{ns} = \sigma^{a}_{ns}/\tau \\ &= (1-\mu_\sigma)\swarrow_{1n}\swarrow_{1s} - (1+\mu_\sigma)\swarrow_{3n}\swarrow_{3s}, \end{aligned} \tag{13}$$

where $\bar{\sigma}^{\alpha}_{ns}$ is the reduced shear stress, acting over fault plane with n in the direction of dislocation vector s, obtained using normalization on τ.

Please cite this article as: Rebetsky, Yu.L., et al., Development of inversion methods on fault slip data, Tectonophysics (2012), http://dx.doi.org/10.1016/j.tecto.2012.09.027

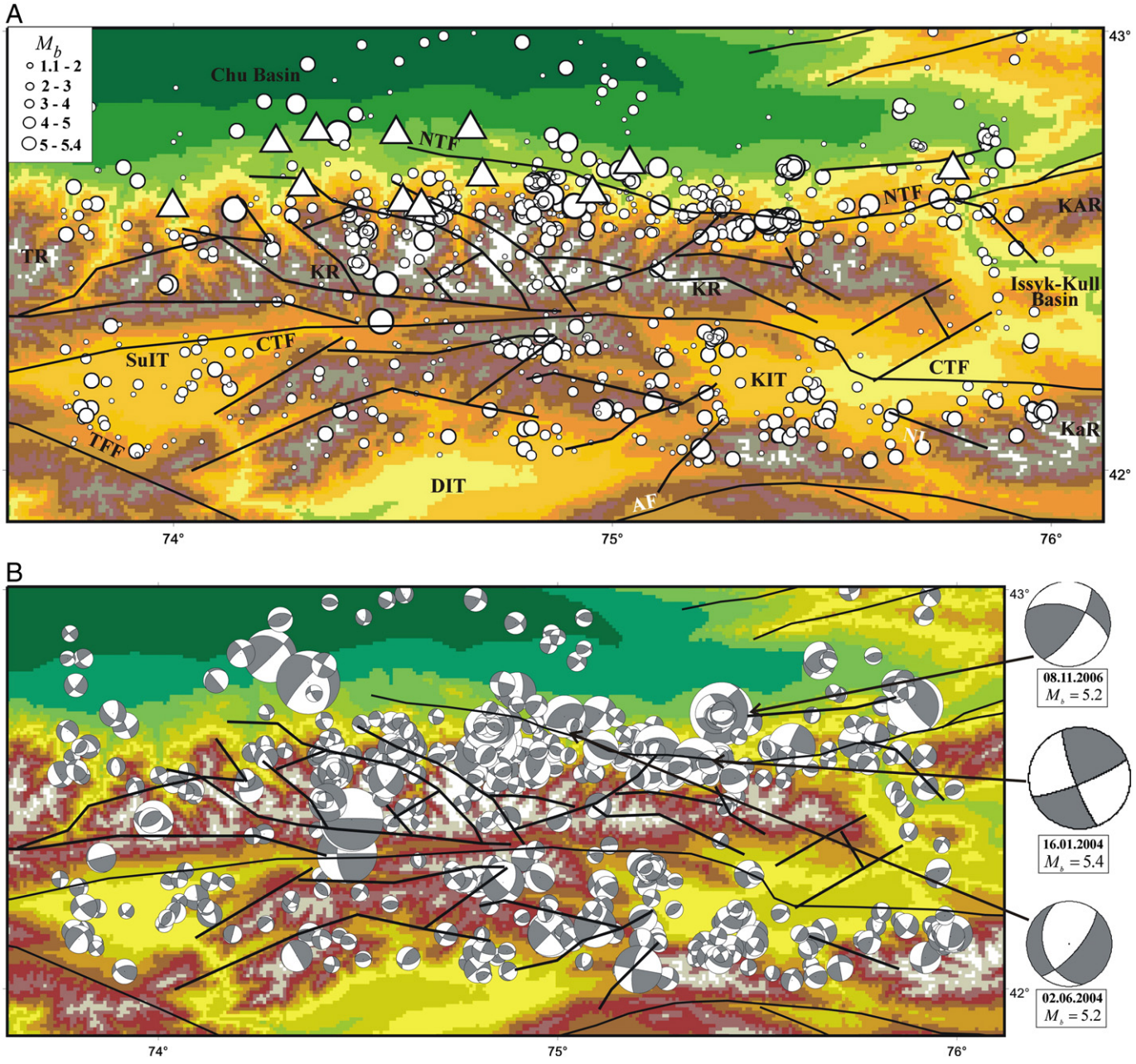

Fig. 7. Tectonic province of Northern Tien Shan orogen. (A) Distribution of earthquake epicenters from catalogue of earthquake focal mechanisms (open circles). Triangles mark the seismic station. (B) Earthquake focal mechanisms of Tien Shan orogen with the range for depth range 5–15 km. $2.5 \geq M_b \geq 5.4$. Earthquakes with $M_b > 5.0$ are taken out for boundary map. Black lines are active faults. Intermontane troughs: DIT — Djumgol, SuIT — Suusamyr, and KIT — Kochkor; Ranges: TR — Talas, KR — Kyrgyz, KAR — Kungei Alatoo, and KaR — Karatoo. Faults: CTF — Central Tien Shan, NTF — Northern Tien Shan, AF — Atbashinskyi, and TFF — Talas Fergan.

Thus, maximum of function (Eq. 13) defines the parameters of normalized stress ellipsoid, for which the sum of normalized projection on dislocation vector of shear stresses acting on fault plans, is maximal. This function, up to normalization on $d\gamma$ and τ, defines dissipation energy of elastic deformations. Trying all values for Lode–Nadai coefficient ($-1 \leq \mu_\sigma \leq 1$) within the area of possible orientation of principal axis one on unit hemispheres can define such orientation of σ_1 and σ_3, for which function (13) gets its maximum.

Note parameters of normalized stress ellipsoid in methods by Angelier (1989a, 1990), Carey and Bruneier (1974), Etchecopar et al. (1981), Gephart and Forsyth (1984) and Nikitin and Yunga (1977) are based on the analysis of unit vectors of dislocation s^α and shear stress t^α on slip fault plane. In these methods different forms of maximum of scalar product are searched:

$$F = \sum_{\alpha=1}^{A} \frac{(s^\alpha t^\alpha)}{|s^\alpha||t^\alpha|}, \tag{14}$$

which actually defines the sum of cosines of angles between axis of dislocation and shear stresses on fault plane. Condition (14) essentially differs from Eq. (13) because it does not see difference for fracture planes close to the plane of maximal shear stresses or to principal axis, where shear stresses are zero.

Please cite this article as: Rebetsky, Yu.L., et al., Development of inversion methods on fault slip data, Tectonophysics (2012), http://dx.doi.org/10.1016/j.tecto.2012.09.027

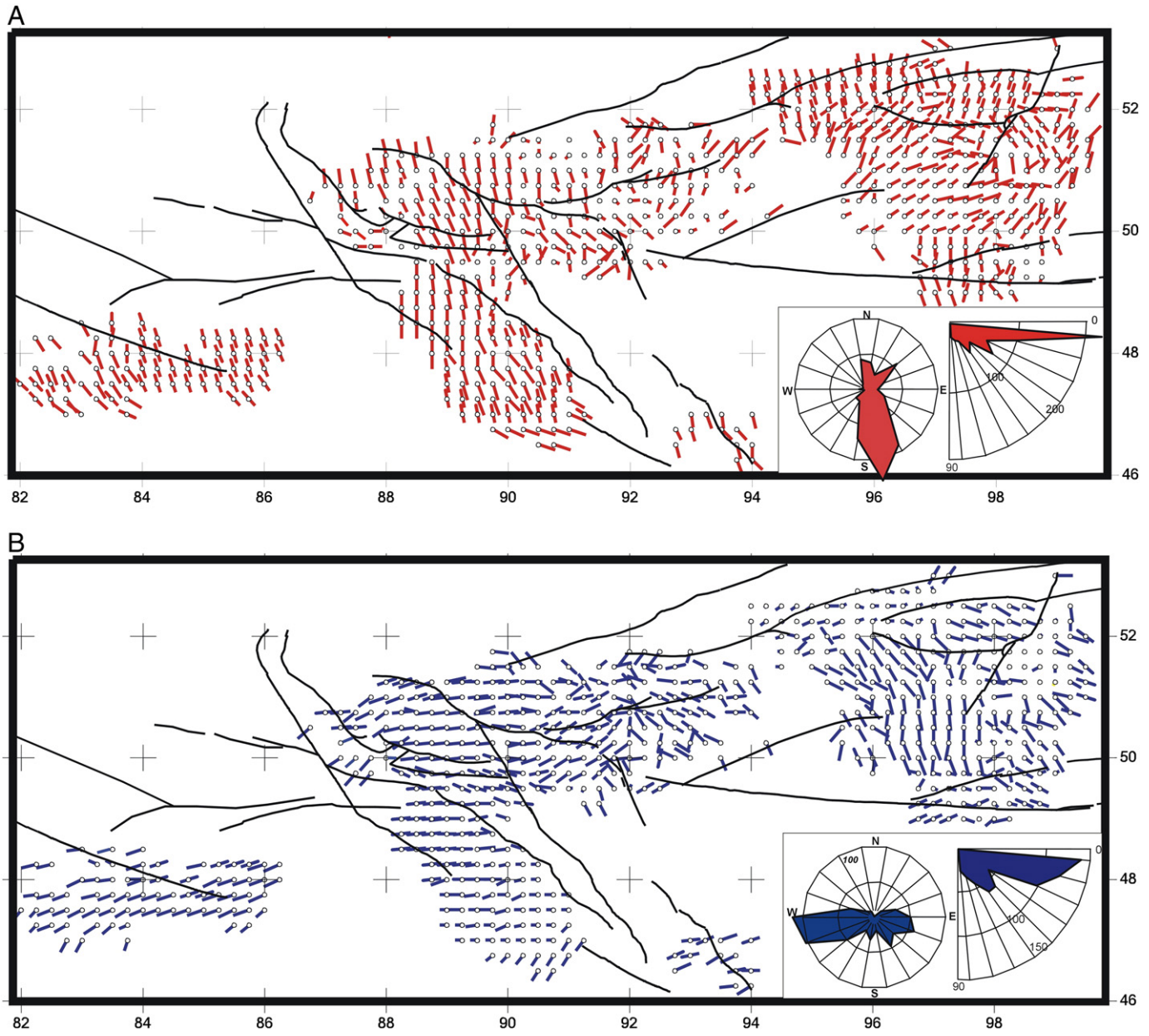

Fig. 8. Projections to a horizontal plane of the plunge axes of principal stresses for Altai and Sayan crust: (A) maximal compression σ_1; (B) algebraically minimal stress (maximal deviatory extension) σ_3. The open circles in the end of an axis mark the beginning of its plunging. In this case an angle of axis plunge more than 15°. Short axes correspond to the big angles of plunge axes. If the open circle is in the middle axis, it means that the angles of plunge axes are less than 15°. Rose diagrams (bottom right corner of the figures) show the predominantly azimuths and plunges of axes of the principal stresses.

Therefore, in the MCA after the first stage of tectonic stress reconstruction, quasi-homogeneous deformed crust domains are recognized. For these domains the loading type is known (orientation of stress principal axis and their relationship) together with set of planes of activated slip faults characterizing the domain. In case of seismological data it is set of nodal planes, one of which is actual plane of slip fault.

The MCA integrates different methods of stress reconstruction (right quadrants and analytical averaging (Angelier and Mechler, 1977; Angelier, 1989a)) and calculation of seismotectonic deformation increment (Riznichenko, 1965; Yunga, 1990). This integration is logical and is based on the fundamental principle of plasticity theory, which recognizes as true stress tensor the one, which supports maximum dissipation of energy of elastic deformations.

2.2. Second stage of the MCA

2.2.1. Fracture zone on Mohr reduced diagram

At second stage of the MCA, fracture zone on Mohr diagram obtained from laboratory experiments (Fig. 3) is used to define τ and p. Experiments on different types of samples (solid media without visible macroscopic defects, with pre-defined macroscopic defects, with cuttings) reported in Byerlee (1968, 1978), Brace (1972), Handin (1969). Mogi (1964), and others demonstrated rather a wide range of scatter on Mohr's diagram (Fig. 3) presenting stress-state on cracks.

All points on Mohr's diagram characterizing critical state on newly developed and re-activated cracks fall into the area between upper yield envelope (inner brittle strength) and bottom line of resistance

Please cite this article as: Rebetsky, Yu.L., et al., Development of inversion methods on fault slip data, Tectonophysics (2012), http://dx.doi.org/10.1016/j.tecto.2012.09.027

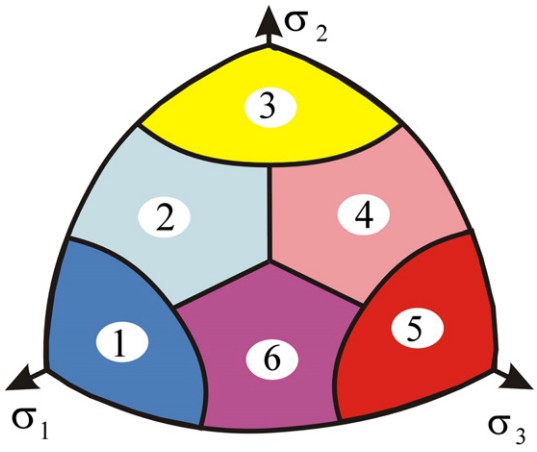

Fig. 9. Types of geodynamic regimes, axis on Zenith is inside one from six sites of spherical octant, formed by three principal stress axes: 1 — the horizontal extension regime (axis σ_1 is sub-vertical); 2 — the horizontal extension with horizontal shear; 3 — the horizontal shear regime (axis σ_2 is sub-vertical); 4 — the horizontal compression with horizontal shear; 5 — the horizontal compression regime (axis σ_3 is sub-vertical); and 6 — the vertical shear stress state (axis σ_2 is sub-horizontal, and σ_1 and σ_3 have angles of axes plunges near 45°).

to static friction with minimal zero cohesion. This can be formalized in the form of inequalities for Coulomb's stress (Byerlee, 1968, 1978):

$$C = \tau_n - k_s\sigma^*_{nn} \geq 0 \text{ and } C = \tau_n - k_f\sigma^*_{nn} \leq T_f \text{ where } \sigma^*_{nn} = \sigma_{nn} - p_{fl}, \quad (15)$$

where $\tau_n \geq 0$ and $\sigma_{nn}{}^* \geq 0$ are shear and effective normal stresses respectively corresponding (Terzaghi, 1943) on the crack plane with normal n; p_{fl} is the fluid pressure in cracks and pores in the rock massive; $T_f(\sigma_{nn}{}^*)$ and $k_f(\sigma_{nn}{}^*)$ are maximal cohesion strength and coefficient of inner friction respectively, in general case depending on effective normal stress; and k_s is coefficient of static friction. The space on Mohr's diagram limited by inequalities (Eq. (6)) can be referred as *brittle fracture zone*. Regularity, depending on which the points on Mohr's diagram fall into the fracture zone, is used at the second stage of the MCA to determine relationships between spherical and deviatory components of sought-for stress tensor.

Within this postulate we assume stress-state critical: Mohr's big circle touches the yield envelope, presenting inner strength (hypothesis 4). This assumption takes into account the fact that reconstruction of stress-state is carried in seismoactive regions, where there are numerous active faults. Therefore, according to Eq. (15), for activated or newly generated fault there is a constraint for Coulomb's stress:

$$\tau^\alpha_n - k_s\left(\sigma^\alpha_{nn} - p_{fl}\right) = T^\alpha_n \text{ where } 0 \leq T^\alpha_n \leq T_f. \quad (16)$$

Here $\tau^\alpha_n = \sigma^\alpha_{nt}$ is the complete shear stress on the crack plane having number α from homogeneous sample. T^α_n is the strength of cohesion for this crack, vector n^α defines the normal to the crack plane, and t^α is the direction of shear stresses for this plane.

According to Eq. (16) as starting point we take the middle part of Mohr's diagram (Fig. 3B) where both limiting lines of inner strength and static frictions are parallel. T^α_n can have different values along differently oriented cracks planes but not exceeding limiting effective inner cohesion T_f. Probably T_f can differ for different crust types and has to depend on the history of tectonic development of the region and its current state and for different scales of stress field.

2.2.2. Relative values of stresses

Results of the first stage make it possible to construct the points, which characterize normal and shear stresses on fault planes from homogeneous sample within the Mohr's big circle of sought-for stress state. Because after the first stage we only no know orientation of principal stress axis and the μ_σ coefficient, position of the center of Mohr's big circle $\sigma_O{}^*$ and its radius τ are unknown. In the MCA for the analysis of homogeneous samples of slip fault sets, it is suggested to use Mohr's diagram (Fig. 3B). According to Eq. (4) stresses on the slip fault plane can be represented in the following form:

$$\sigma^{*\alpha}_{nn} = \sigma^*_O + \tau\tilde{\sigma}^\alpha_{nn}; \sigma^\alpha_{ns} = \tau\tilde{\sigma}^\alpha_{ns}, \quad (17)$$

when $\sigma^*_O = p^* + \frac{\mu_\sigma}{3}\tau, p^* = p - p_{fl}, \tilde{}\sigma^\alpha_{ng} = (1-\mu_\sigma)\swarrow^\alpha_{1n}\swarrow^\alpha_{1g} - (1+\mu_\sigma)\swarrow^\alpha_{3n}\swarrow^\alpha_{3g} + \delta_{ng}\mu_\sigma, g = n, s$.

Here $\tilde{\sigma}^\alpha_{ns}$ and $\tilde{\sigma}^{*\alpha}_{nn}$ are the corresponding reduced shear and effective normal (taking into account fluid pressure (Eq. (15))) stresses acting on the crack plane with number α taken from homogeneous sample of slip fault sets; vector s defines the direction of slip along the crack plane, and δ_{ng} is the Kronecker delta. Note that here, we, for the moment, assume that we know the acting fault plane in case of seismological data on earthquakes source mechanism.

These reduced stresses are completely defined after the first stage. On the reduced Mohr's diagram big circle has a unit radius (all parameters are normalized on maximal shear stress τ value), and its center coincide with the beginning of the coordinate system (shifted to the left by $\sigma_O{}^*$ value, see Fig. 3B). Using such reduced Mohr's diagram (Fig. 3B) we analyze homogeneous sample of slip faults. Through each point characterizing stresses it is possible to plot a line parallel to the yield strength line and the line of static friction with zero cohesion. For calculations it is used a point, for which length of the perpendicular plotted from the center of Mohr's big circle is minimal. Note, this actually means the assumption that in the sample set there is at least one activated crack with zero cohesion (hypothesis 5). For such point it is assumed that strength of surface anchoring is equal to zero ($T^K_n = 0$). Then, using scheme plotted in Fig. 3B and expressions (16) and (17), we find the ratio of effective confining pressure to the module of maximal shear stress (Rebetsky, 2005a, 2007):

$$\frac{p^*}{\tau} = \frac{1}{k_s}\left(\tilde{\sigma}^K_{ns} - k_s\tilde{\sigma}^K_{nn}\right) - \frac{\mu_\sigma}{3}, \text{where } \tilde{\sigma}^k_{ns} = \tilde{\tau}^k_n. \quad (18)$$

For the point B, where the line of maximal strength of rocks is tangent to the Mohr's circle, the limiting relationship (Eq. (16)) is valid, formulated for maximal cohesion value T_f. Based on it together with Eq. (17) and the scheme presented in Fig. 3B, one can get:

$$\tau/T_f = \frac{1}{\sec 2\phi_s - \left(\tilde{\sigma}^K_{ns} - k_s\tilde{\sigma}^K_{nn}\right)}; p^*/T_f \frac{= \tilde{\sigma}^K_{nt} - k_s\tilde{\sigma}^K_{nn} - k_s\mu_\sigma/3}{k_s\left[\sec 2\beta_s - \left(\tilde{\sigma}^K_{ns} - k_s\tilde{\sigma}^K_{nn}\right)\right]}, \quad (19)$$

where $\beta_s = \frac{1}{2}\arctan\frac{1}{k_s}$. $\phi_s = \arctan k_s$.

Therefore, analyzing the location of points characterizing stress on fault planes from homogeneous sample, one can define that maximal shear stresses τ normalized to unknown value T_f, and effective confining pressure p^*. Correspondingly, all components of effective stress tensor (stresses, taking into account fluid pressure) can be calculated.

It has to be noted that when building the calculation scheme, we made an assumption that activation of slip along fault depends on complete shear stress ($\tau_n = \sigma_{nt} = \sqrt{\sigma^2_{ns} + \sigma^2_{nm}}$), acting on the crack plane in direction of the t^α, though the dislocation itself occurs along the $\mathbf{s}^\alpha$ due to the anisotropy (hypothesis 6). Complete shear stresses acting on the crack plane are responsible for overcoming the friction (destruction of asperities along crack sides, making obstacle for slipping). Hence, expression (19) led us to define the relative values of maximal shear stress and effective pressure for known values of inner cohesion friction and data on orientation of fault planes.

Please cite this article as: Rebetsky, Yu.L., et al., Development of inversion methods on fault slip data, Tectonophysics (2012), http://dx.doi.org/10.1016/j.tecto.2012.09.027

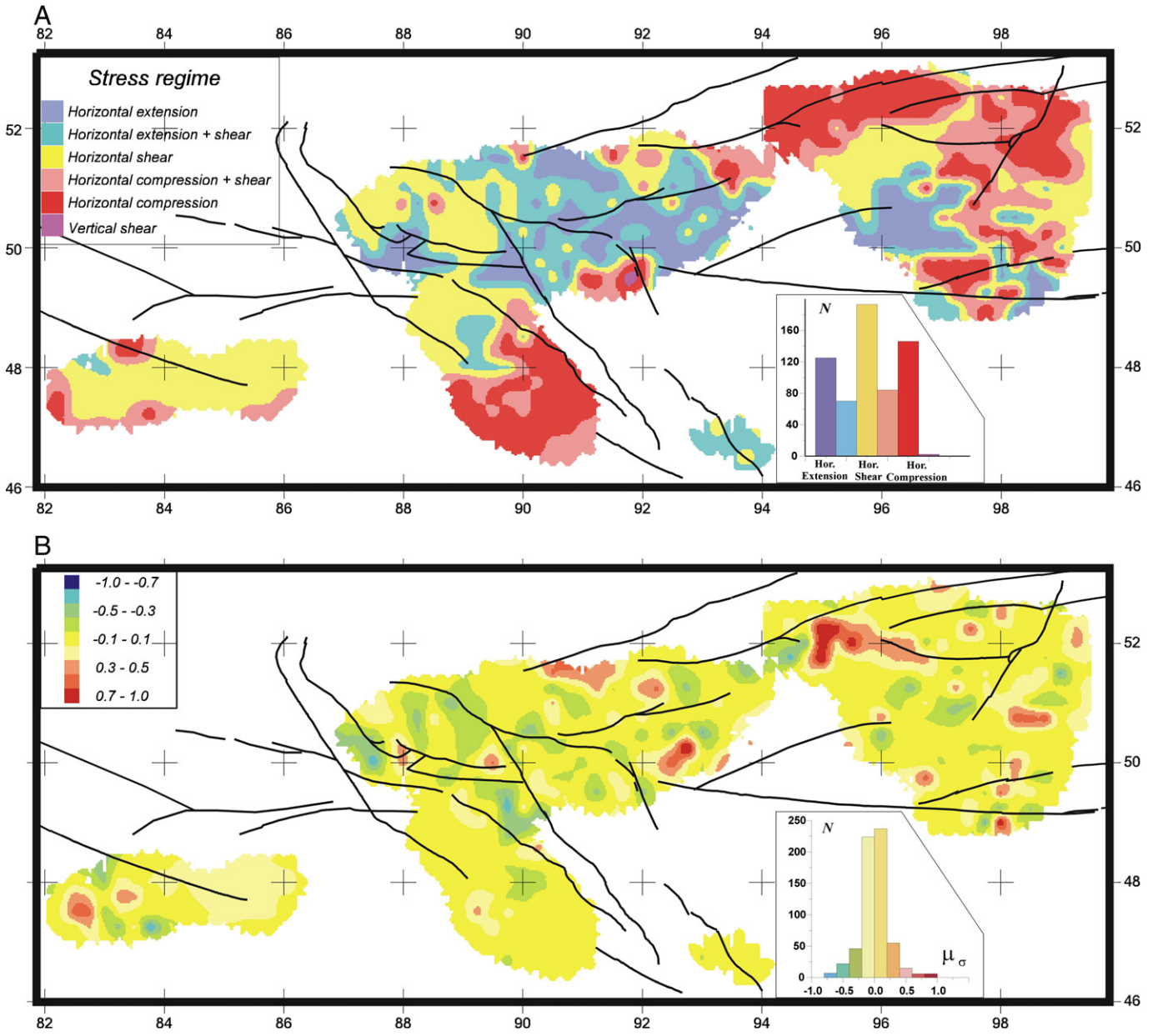

Fig. 10. Types of geodynamic regimes (A) and values of Lode–Nadai coefficient and (B) of Altai and Sayan crust. Prevailing value of parameters shows the diagrams on the bottom right corner of the figures.

In conclusion of this section we mark that concerning the reconstruction of tectonic stresses based on the data on slip fault sets (Gephart and Forsyth, 1984) suggested for the first time to analyze relative values of principal axis based on character of distribution of points on Mohr's diagram, which defines normal and shear stresses on a crack plane. They propose drawing a line of effective strength through the areas of maximal density of such points on the diagram. In frames of proposed method it is possible to get dimensionless values of principal stresses. In two examples presented in this study the ratio τ/p^* was taken to be 0.86 (model A) and 1.34 (model B). Similar approach was proposed also in Michael (1984). In that paper it was introduced additional assumption on one of the principal stress axis being sub-vertical.

The approach developed by Angelier (1989b) is the one closest to the described algorithm of the second stage of the MCA. Also in Angelier's method a postulate is used that the points characterizing shear and normal stresses of cracks composing homogeneous sample fall in fracture zone, which is constructed using results of experiments by Byerlee (1968, 1978). From the slope of the bottom of point's cloud, which defines the minimal static friction, coefficient of surface friction is defined; ratio of complete components of maximal and minimal pressure is determined on the basis of hypothesis 6. Results of calculations for geological data on shear cracks in the region near Hover dam in the USA demonstrate that coefficient of friction is close to 0.51 and the ratio $\Psi = \sigma_3/\sigma_1$ is close to 0.06.

2.2.3. Recognition of earthquake source plane

The MCA algorithm of evaluation of relative stress values (Eq. (19)) is based on the knowledge of crack plane orientation. It is always the case when analyzing geological data on striation traces. For seismological data on nodal plane solutions we do not know, which one of two nodal planes was realized as fault. The MCA is

Please cite this article as: Rebetsky, Yu.L., et al., Development of inversion methods on fault slip data, Tectonophysics (2012), http://dx.doi.org/10.1016/j.tecto.2012.09.027

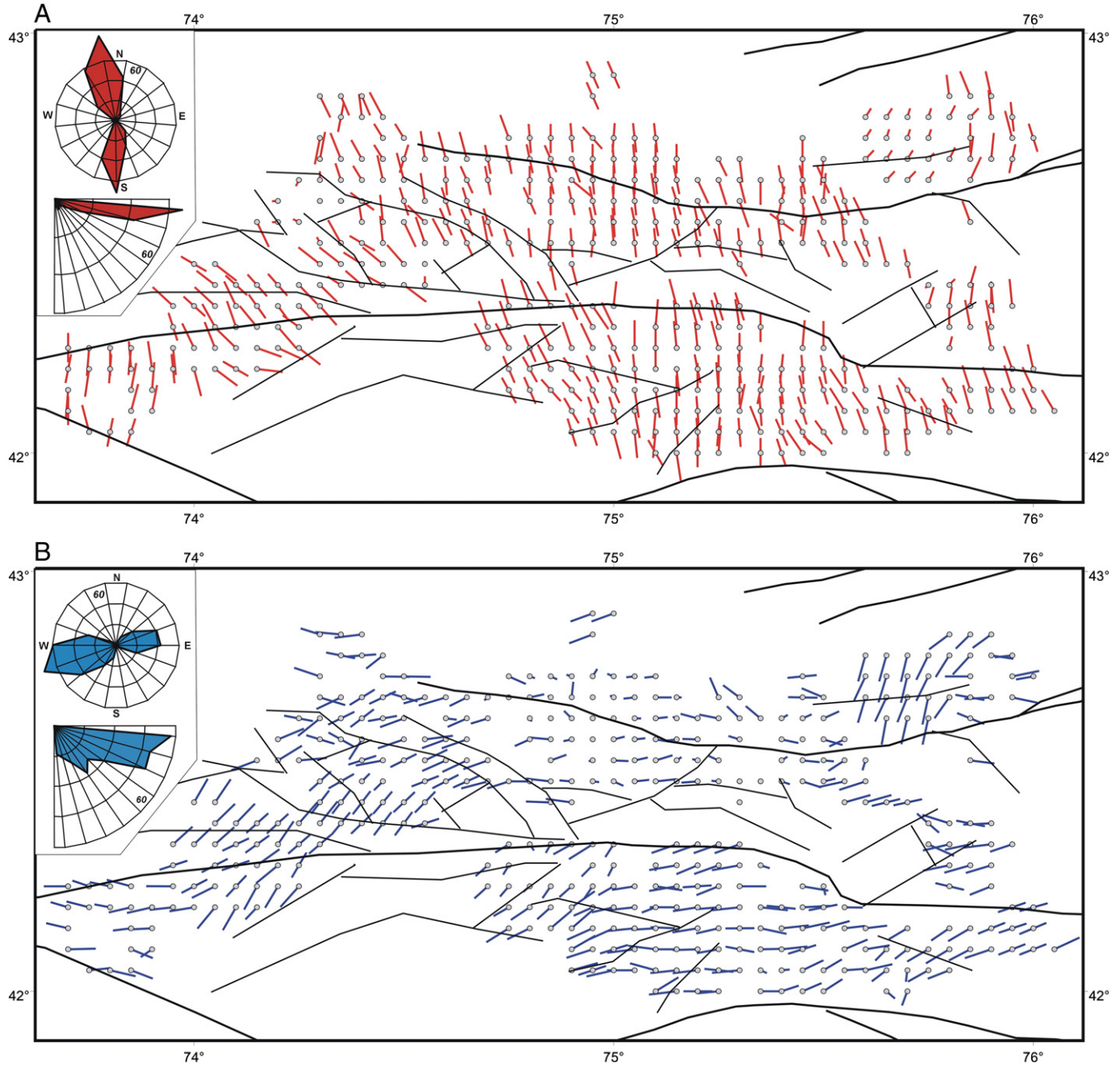

Fig. 11. Projections to a horizontal plane of the plunge axes of principal stresses for Tien Shan crust: (A) maximal compression σ_1 and (B) algebraically minimal stress σ_3. Black lines are active faults.

developed as a procedure for the identification of the actual fault plane in the earthquake source. The plane for which Coulomb stress C is higher is selected as the actual fault plane between two nodal planes (hypothesis 7):

$$MAX\left[C_n^\alpha \;;\; C_s^\alpha\right] \text{ where } C_n^\alpha = \tau_n^a - k_s\sigma_{nn}^\alpha,\;\; C_s^\alpha = \tau_s^\alpha - k_s\sigma_{ss}^\alpha. \tag{20}$$

Here τ_n^α and $\sigma_{nn}^{*\alpha}$ are shear and normal stresses acting on nodal plane with normal n^α; τ_s^α and $\sigma_{ss}^{*\alpha}$ act on the nodal plane with normal s^α.

According to Eq. (20) nodal planes supplying points in the upper left part of the complete Mohr's diagram are preferable when choosing the nodal plane. In case when nodal planes are close to the planes of maximal shear stresses, criterion (20) has only formal meaning because corresponding points on Mohr's diagram almost coincide located near the vertical axis τ_n.

Displacement in the source may not coincide with direction of shear stresses. In Eq. (20), let us replace shear stresses acting on τ_n^α and τ_s^α planes by shear stress σ_{ns}^α, which acts along the nodal plane in the direction of dislocation. From such modification of Eq. (20) it follows that in the MCA the actual plane is selected the one for which confining pressure and friction forces are smaller.

Analysis of the Spitak, 1988, earthquake ($M_b = 6.9$) sub-sources demonstrates the use of criterion (20). Mechanisms and location of the sub-sources and the first strong aftershock (F) are shown according to Arefiev et al. (2005). Results of the first stage of reconstruction were done according to the Harvard CMT solutions making it possible to define the orientation of regional stress principal axis:

Please cite this article as: Rebetsky, Yu.L., et al., Development of inversion methods on fault slip data, Tectonophysics (2012), http://dx.doi.org/10.1016/j.tecto.2012.09.027

azimuth and dip of σ_3 are correspondingly 252° and 6°, and for σ_1 — 157° and 37° (Rebetsky, et al., 2001) Coefficient of the stress tensor shape is $\mu_\sigma \approx 0.3$. Analysis of acting planes in sub-sources is shown in Fig. 4B. All planes, selected as actual fault planes based on analysis of the aftershock sequence (Arefiev et al., 2005), satisfy criterion (20). It is clear that vectors of reduced stresses define location of points close to the Mohr's big circle, and almost all except number four nodal planes auxiliary to the acting ones are concentrated in the central part of the diagram.

Different selection algorithms of acting nodal plane based on seismological data were proposed in studies devoted to reconstruction of principal stress axis. In Nikitin and Yunga (1977) it was suggested to choose as acting plane the nodal plane for which projection of shear stress along direction of dislocation vector is maximal. Because stress values are unknown, in calculations shear stresses are normalized on unknown value of maximal shear stress τ (see expression (4)). It means that it is selected a plane for which the difference between reduced shear stress acting on it and shear stress in slip direction

$$\Delta_n^\alpha = \bar{\tau}_n^\alpha - \bar{\sigma}_{ns}^\alpha, \quad \Delta_s^\alpha = \bar{\tau}_s^\alpha - \bar{\sigma}_{ns}^\alpha \text{ for } \bar{\sigma}_{ns}^\alpha = \sigma_{ns}^\alpha/\tau, \text{ and } \bar{\tau}_i^\alpha = \tau_i^\alpha/\tau \ (i = n, s) \tag{21}$$

is minimal.

Selection algorithm by Gephart (1985) and Gephart and Forsyth (1984) is similar to Eq. (21) but amplitudes of relative shear stresses are not considered. It is proposed to select the nodal plane for which the angle between vectors t^α and s^α or t^α and n^α is minimal (see expression (13)).

In frames of kinematic approach (Gushchenko and Kuznetsov, 1979; Lisle, 1987) selection criteria of acting plane from homogeneous sample is:

$$\measuredangle_{1j}^\alpha \ \measuredangle_{3j}^\alpha \ \measuredangle_{1m}^\alpha \ \measuredangle_{3m}^\alpha > 0, j = n, s, \tag{22}$$

where $\measuredangle_{kn}^i$ and $\measuredangle_{ks}^i$ are direction cosines normal vectors n and s to nodal planes, and $\measuredangle_{mk}^i$ ($k = 1, 3$) are direction cosines of vector m in slip fault plane and orthogonal to the slip vector s in coordinate system referenced to principal axis of sought-for stress tensor.

Comparison of algorithms for selection of nodal planes based on earthquake source mechanisms demonstrates that criteria (21) and (22) choose the planes which points are distributed over all area of big circle. Criterion (20) makes a choice of the planes, stress-state on which is mostly in the left side of the Mohr's big circle. It corresponds better to the assumption that rock failure is governed by the Coulomb–Mohr law.

Note that in the algorithm of the second stage of the MCA value of friction coefficient k_s is evaluated. For this purpose the slope of the bottom margin of distribution of points, characterizing stresses on discontinuities on summary Mohr's diagram for all homogeneous samples of the region is analyzed, as Angelier (1989b) did it. Based on the analysis for Altai and Sayan region the coefficient is evaluated to be 0.5 and 0.6 for Central Tien Shan.

3. Stress-state of the crust in the Central Asia orogens

3.1. Seismotectonics of the Central Asia

Orogens of Tien Shan, Altai, and Sayan compose the core of the mountain belt of Central Asia (Fig. 5). The generally accepted assumption is that the uplift of the mountains is result of Indian and Eurasian plate collision occurred 45 million years before present.

Alati and Sayan mountains (Fig. 6A) are part of the Urals–Mongolian (Central Asian) folded belt extending from Urals up to Pacific coast. It lies between mountain systems of Pamir and Tien Shan and platform system bordering with the Baikal rift. Starting from middle Triassic (245 million before present) weak and moderately differentiated movements dominated in the Altai–Sayan region. They smoothed contrast Paleozoic topography and developed alluvial deposits. As a modern mountain domain Altai and Sayan was formed in Cenozoic (Oligocene, 33–25 million years bp.) at the place of planes and hills. Cenozoic activation is expressed by accumulation of Neocene–Quaternary continental glacial, lake, and alluvial deposits in the Zaisan, Chuya, Ubsunur, Jungar and other depressions. Midland and highland topographies were formed in the zones of modern arch-block uplifts of the Gorniy Altai (Trifonov et al., 2002).

Altai–Sayan region is seismically active. There frequently occurred strong earthquakes, in particular: Mongolian (1761, $M = 7.7$.), Tsetserlic and Bolnai (1905, $M = 7.6$, $M = 8.2$), Mongol–Altai (1931, $M_b = 7.9$), Ureg–Nur (1970, $M_b = 7.0$), Zaisan (1990, $M_b = 6.9$), Busingol (1991, $M_b = 6.5$), and Chuya (2003, $M_b = 7.3$), which have left pronounced traces on the surface (Fig. 6B).

The catalogue of fault-plane solutions in 1963–2003 includes 308 events. Fault plane solutions are based on the first-motion sign. Solutions are reliable for $M > 4.5$, when number stations used from 35 to 80 seismic stations. Less accurate are solutions for smaller earthquakes, when data from 10–30 stations are used (Soboleva et al., 1980; Solonenko et al., 1993). First motion signs were collected from Altai and Baikal seismic networks augmented by the data from Kazakhstan and China. Earthquake mechanisms are of various types. Combination of thrust and strike–slip mechanisms is characteristic of mountain ranges. In large depressions normal faulting together with normal–strike–slip mechanisms are observed often. In the region, 16 solutions are available from Harvard CMT catalogue.

Longitudinally elongated Central and Eastern Tien Shan is highly deformed region jammed between two rigid blocks of the earth crust: Kazakhstan platform in the north and Tarim depression in the south. The topography of Central Tien Shan is presented by ranges and depressions formed by folding and thrust tectonics (Fig. 7). It is assumed that Tien Shan structure is developed under latitudinal horizontal shortening starting from Oligocene (Makarov, 1977; Nikolaev, 1988). The average rate of uplift during Oligocene–Quaternary was less than during Quaternary and late Pleistocene, (Chediya, 1986; Krestnikov et al., 1976; Trifonov et al., 2008). Presence of longitudinal left and right lateral shear zones in modern Tien Shan structure (Buslov et al., 2003; Cobbold and Davy, 1988; England and Molnar, 1997; Makarov, 1977) lets us consider it as trans-press zone.

The KNET network was installed in 1991. It includes ten digital broadband stations. The hypocenter (Lienert et al., 1986) and velocity model by S.W. Roecker et al. (1993) is used for hypocenter location. The program not only locates the hypocenter but also generates file, which can be used further to get fault plane solutions. The mean RMS is ca. 0.2–0.3 s, which ensures location accuracy of 1.2–1.8 km. The essential requirement for correct fault-plane solution is good station coverage. Taking into account the geometry of the network, we evaluate the well-controlled region in the spatial frames 42°–43°N and 73.75°–76°E. The *Fpfit* (Reasenberg and Oppenheimer, 1985) software is used for fault-plane solutions. The catalogue of focal mechanisms for time-interval 1999–2008 includes 800 earthquakes (Sychev et al., 2003; Sycheva et al., 2009).

The earthquake sources of the northern Tien Shan are located within the crust, more precisely in its upper part in pre-Mesozoic basement. Central Tien Shan is characterized by different types of earthquake mechanisms, but the dominant one is thrusting (Fig. 7), with compressure axis of earthquake mechanism sources oriented horizontally in the north-east direction.

3.2. Results of stress ellipsoid calculations

3.2.1. Altai and Sayan regions

The preliminary analysis shows that the spatial and magnitude distribution of earthquake sources make it possible to reconstruct the stresses averaged within 50–70 km in lateral direction and for

Please cite this article as: Rebetsky, Yu.L., et al., Development of inversion methods on fault slip data, Tectonophysics (2012), http://dx.doi.org/10.1016/j.tecto.2012.09.027

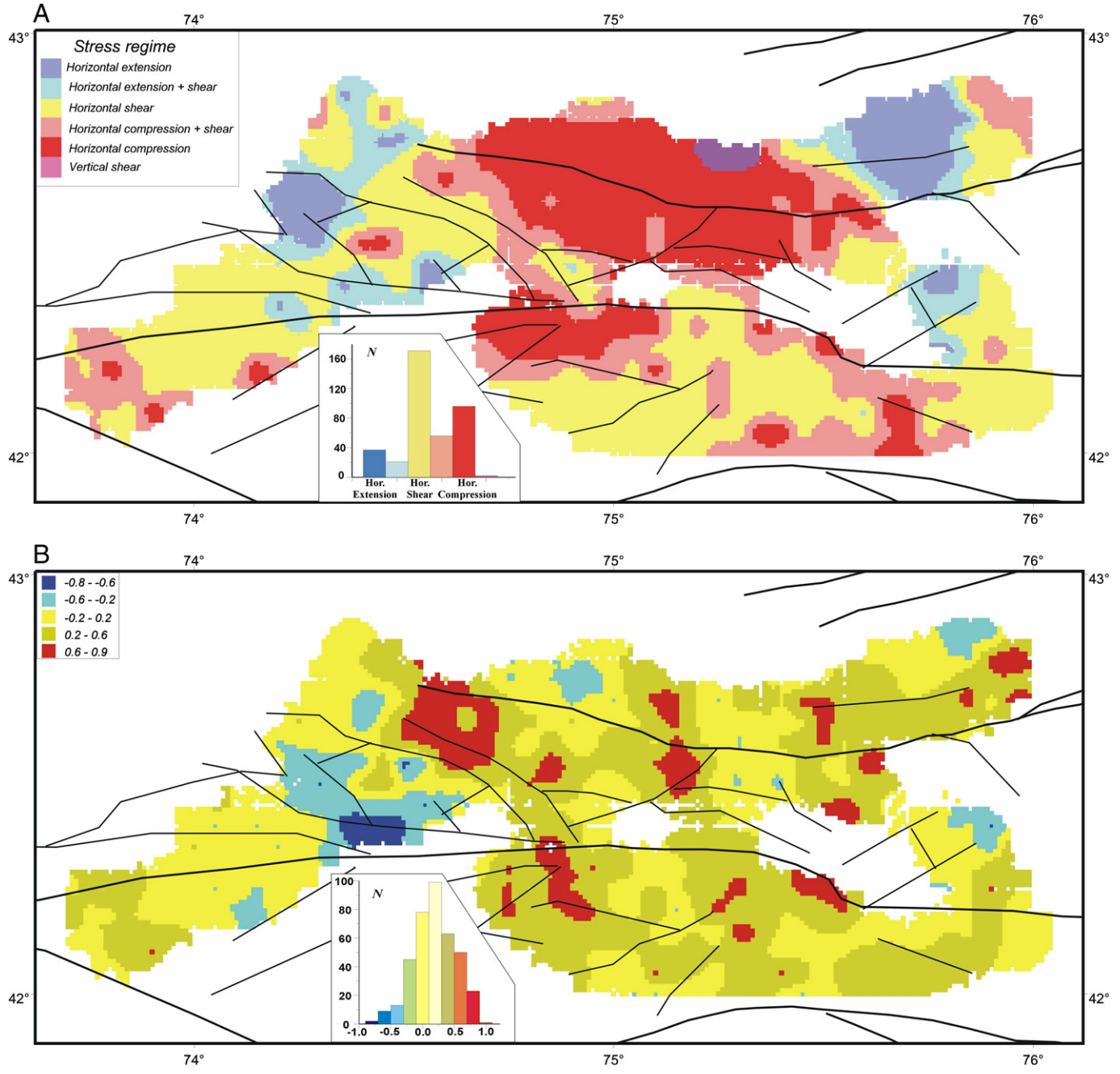

Fig. 12. Types of geodynamic regimes (A) and values of Lode–Nadai coefficient and (B) upper part of the Northern Tien Shan crust.

the whole crust thickness. This averaging scale is comparable with transversal size of some ranges and depressions. That is why in the gradient stress field reconstructed stresses could be assigned to neighboring crust domains, even if they really are in the intermediate stress state. To reduce this negative effect the grid size was chosen to be 0.25°×0.25° located at 15 km depth. Finally the number of quasi-homogeneous domains is 620, each one including at least 6 earthquakes.

The most stable feature of reconstructed maximum compression stress axis σ_1 in the western part (Zaisan valley, Gorny and Mogolian Altai) is its SSE orientation, gently dipping (Fig. 8A). Similar orientation of σ_1 axis is characteristic also in northern and southern parts of the Eastern Sayan. Sub-vertical orientation of σ_1 corresponds to large sedimentary basins and inter-mountain valleys (central part of Tuva and Ubsu–Nur basin and western part of Tuva–North Mongolian Massive). Axis of principal stress σ_3 in most of the regions is sub-horizontally oriented along NNW (Zaisan valley), along latitude (Gorny and Mongolian Altai), and in SSW direction (Tuva–North Mongolian Massive). Orientation of σ_3 axis is very variable in Tuva and Ubsu–Nur basins and also in surrounding Tannoul uplift and Khingan anticlinorium (Fig. 8B). There are also some regions where the orientation of the axis is sub-vertical.

Data on orientation of principal stress axis make possible regionalization of the earth crust based on its geodynamic or stress-state regimes. It is defined by mutual orientation of principal stress axis and zenith direction. Six zones of the octant composed by dividing great arc on 30° and proximity of the axis to zenith are shown in Fig. 9.

Almost all possible states from horizontal compression up to horizontal extension are observed within the region of study (Fig. 10A). The dominant type of the stress state is horizontal shear and its

Please cite this article as: Rebetsky, Yu.L., et al., Development of inversion methods on fault slip data, Tectonophysics (2012), http://dx.doi.org/10.1016/j.tecto.2012.09.027

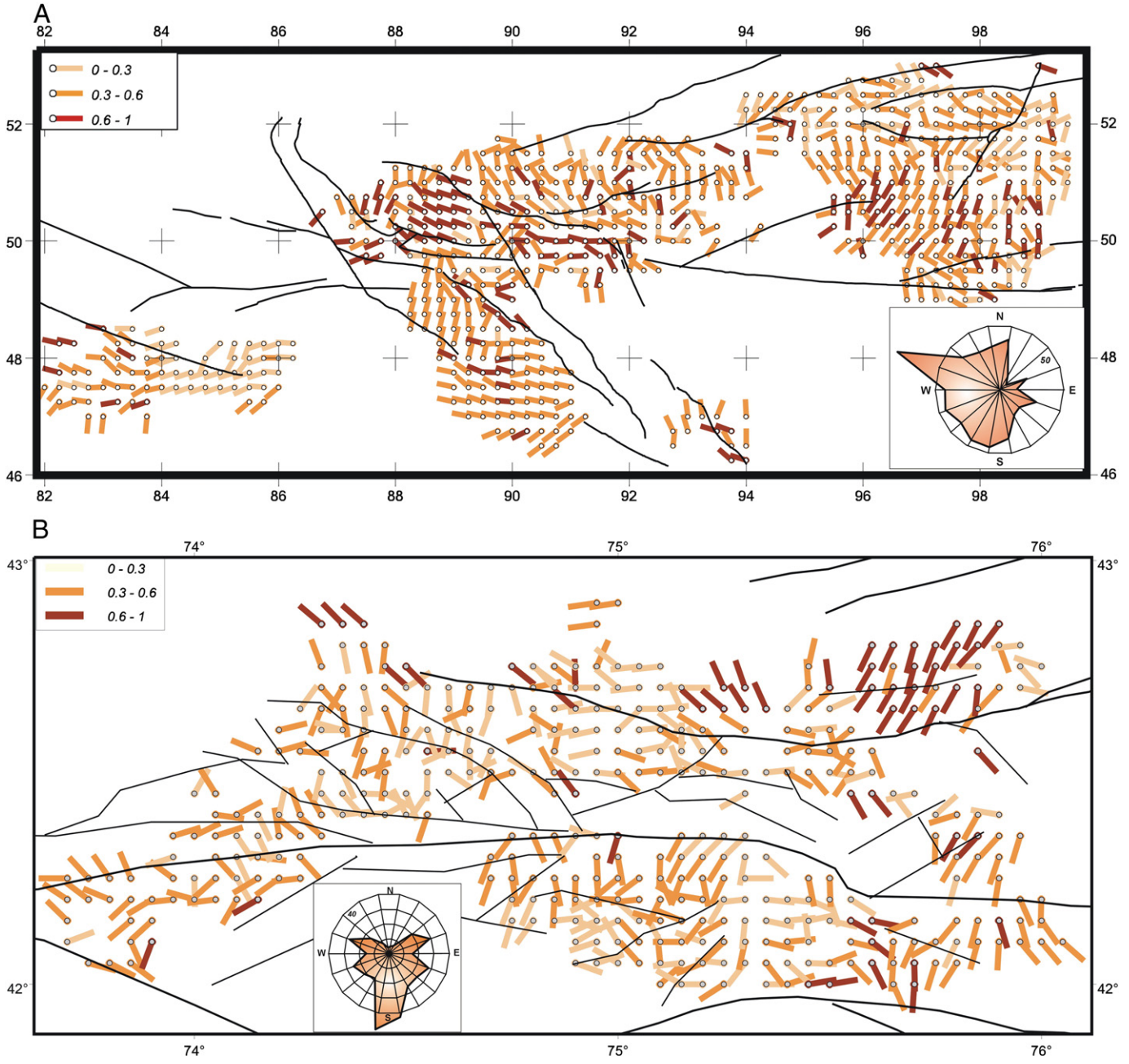

Fig. 13. Directions of underthrusting shear stresses τ_z over the horizontal plane with a normal to the center of the Earth and their relative value (reduced by maximum shear stresses τ_z/τ). Rose diagrams (bottom right corner of figure) show the predominantly azimuths of shear stresses τ_z. (A) Crust of Altai and Sayan and (B) crust of Northern Tien Shan.

combination with horizontal compression and extension. Local segments of horizontal extension are observed in the crust in North Chuya Range and near Kobdo and Shagshal Faults.

Note that all segments of horizontal compression are confined within uplifts and most of segments of horizontal extension are within large valleys. The crust in Western Sayan is mostly characterized by horizontal extension excluding central and eastern parts of Tuva basin, where the horizontal compression is observed. Horizontal extension is found in Eastern Sayan, in western and eastern parts of Tuva–North Mongolian Massive. There are also region of pure horizontal shearing (Zaisan basin, Gorny Altai, eastern part of Tuva basin, etc.).

Lode–Nadai μ_σ coefficient almost everywhere corresponds to stress tensor of pure shearing (deviatory stresses of maximum compression and tension have almost equal absolute values) excluding some places. The largest one among these exceptions is transition zone from Tuva basin toward central zone of Eastern Sayan (Fig. 10B). Stress tensor type there corresponds to uniaxial compression (absolute value of deviatory compression is two times larger than the other two principal stress axis, which have almost the same value).

3.2.2. Upper part of the crust of the Northern Tien Shan

Analysis of the spatial and magnitude distribution of the fault plane solutions demonstrated that the scale for averaging the reconstruction of stresses corresponds to 10–15 km. As a result the grid size is taken equal to 0.05°×0.05° and 5 km in depth. The stress parameters were determined for 283, 384, 328, and 176 domains at 5, 10, 15 and 20 km correspondingly. We present here the result for the depth level 5–15 km (the grid is located at 10 km depth). In the

Please cite this article as: Rebetsky, Yu.L., et al., Development of inversion methods on fault slip data, Tectonophysics (2012), http://dx.doi.org/10.1016/j.tecto.2012.09.027

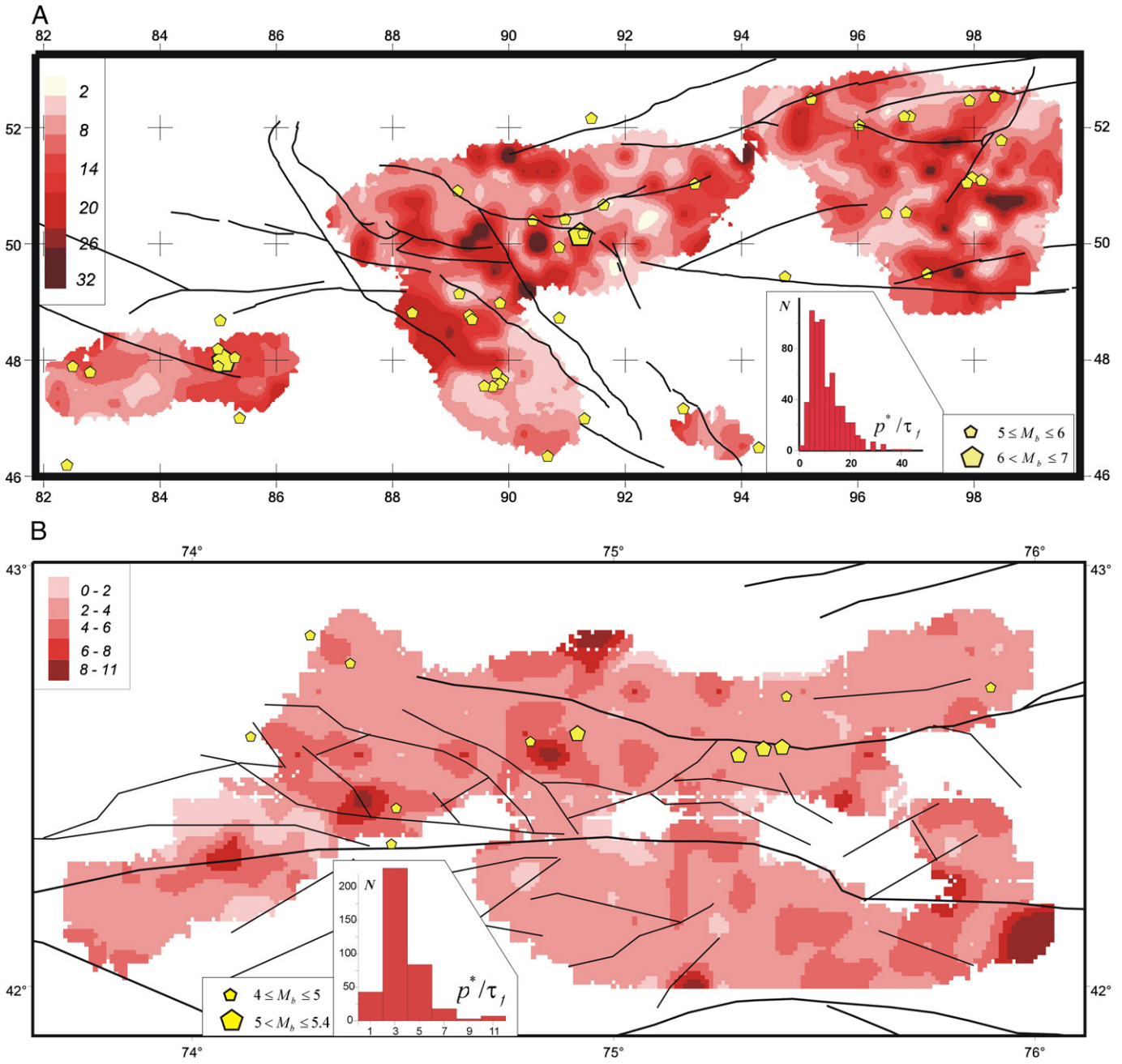

Fig. 14. Relative effective isotropic pressure p^*/τ_f for earth crust of Altai–Sayan (A) and Northern Tien Shan crust (B). Pentagons correspond to the stress states of domains where there were strong earthquakes.

homogeneous set of the mechanisms each one contains more than six events.

Reconstruction revealed that direction of maximal compression stress axis σ_1 is mostly toward NNW (Fig. 11A). The dipping of the axis is from to the south to the north in different areas of the region. There are also domains, where the axis oriented sub-vertically. They correspond to the eastern segment of Chuya depression where Kirgiz Range is merged with Nikdyntas Mountains and also to its northern slopes where Chuya depression cuts it. Axes of principal stress σ_3 are mostly oriented sub-latitudinal diverging toward SW in Azhugaitai and Susamyr ranges and western part of Cuya depression (Fig. 11B). Sub-vertical orientation of the axes is found in the central part of the region.

Part of the region is characterized by horizontal shearing under wide range of horizontal pressure regimes (Fig. 12A). Besides these two types of geodynamic or stress-state regimes of horizontal extension are found, where the axes of maximum compression are oriented sub-vertical. As it has been already marked, these areas are associated with Chuya depression cutting mountains and with crust within intermountain valleys.

In contrast to Altai and Sayan mountains, within the central Tien Shan crust there are large spatial domains where the Lode–Nadai coefficient is nearly $+1$ or -1. These values indicate regimes of uniaxial tension or compression correspondingly (Fig. 12B). Most of the region is characterized by nearly zero value (0.2 to -0.2) or close to it (± 0.4).

3.2.3. Underthrusting shear stresses

Information on the orientation and the shape of stress ellipsoid obtained on the first step of interpretation makes it possible to define the orientation of the shear stresses acting over horizontal planes.

Please cite this article as: Rebetsky, Yu.L., et al., Development of inversion methods on fault slip data, Tectonophysics (2012), http://dx.doi.org/10.1016/j.tecto.2012.09.027

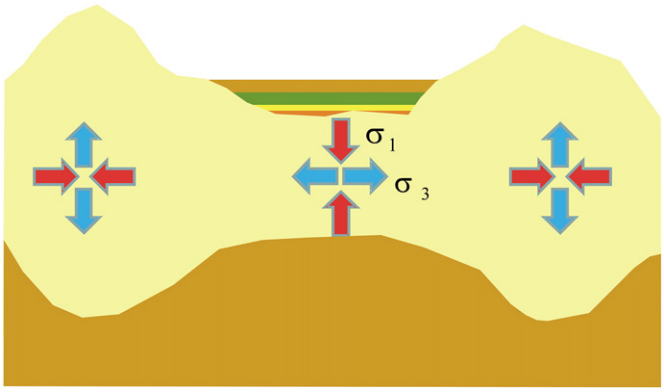

Fig. 15. The generalized scheme of distribution of stress state regimes in the crust of intra-plate fold and thrust belt in Central Asia. 1 — crust, 2 — mantle, and 3 — sedimentary.

This is underthrusting shear stresses. The experience gained in subduction zones (Rebetsky, 2009c; Rebetsky and Marinin, 2006a,b) has demonstrated that the orientation of underthrusting shear stresses is in good agreement with the hypothesis of convection mechanism, with which mantle acts on the lithosphere. One can expect that the pressure caused by the Indian plate will result in pure shearing in the vertical plane oriented from north to south for highland regions as consequence of resistance of continental crust to the deformation of mantle beyond lithosphere. But the result of reconstruction demonstrates that the direction of underthrusting shear stresses is highly variable (Fig. 13) and their intensity (normalization is made on the unknown value of maximal shear stresses) does not depend on the distance between the crust domains from the collision zone of the Indian plate.

It has to be noted that higher values of these stresses are found more often in the crust of highlands (Gorny and Mongolian Altai, Tuva–North Mongolian Massive) and mountain ranges of Altai Sayan(Fig. 13A), and lower values are in basins (Zaisan, Tuva). Circa 90% of acting underthrusting shear stresses is mutually compensated. Such distribution of underthrusting shear stresses reflects the small effect which the mantle has on the crust in the region, at least because of its lateral movement. Data on orientation of such underthrusting shear stresses only show the general direction of mantle movement relative to the crust in WNW (diagram on the Fig. 13).

Underthrusting shear stresses for reflecting impact of the mantle acting on the horizontal planes within the crust of Northern Thin Shan have quite a mosaic distribution (Fig. 13B). Almost 90% of the tangential stresses are mutually compensated. As for Altai and Sayan, data on the orientation of underthrusting shear stresses in Tien Shan indicate general direction of mantle movement relative to the crust toward WSW.

3.3. Relative values of stresses in Central Asia

The second stage of reconstruction within the MCA reveals inhomogeneous distribution of maximum shear stresses τ and effective confining pressure p^*. Hereafter effective confining pressure is defined as the difference between pressure in the rocks p and pressure of fluids p_{fl} in the pores and cracks.

Large domains of high effective pressure extend along Kobdo fault within Gorny Altai and Alash fault in western Sayan. In Mongol Altai, effective pressure decreases from north to south (Fig. 14A). In Eastern Sayan higher values of effective pressure are associated with the Belin–Businggol sub-meridian fault system and latitudinal Academic Obruchev fault.

Spatial distribution of stress values in Northern Tien Shan, as well as in Altai and Sayan, is a mosaic. Areas with high level of maximum shear stress and effective pressure having dimensions 100 over 100 km are in contact with the areas where the level of stresses is two times less (Fig. 14B). Here as in Altai and Sayan the earthquakes

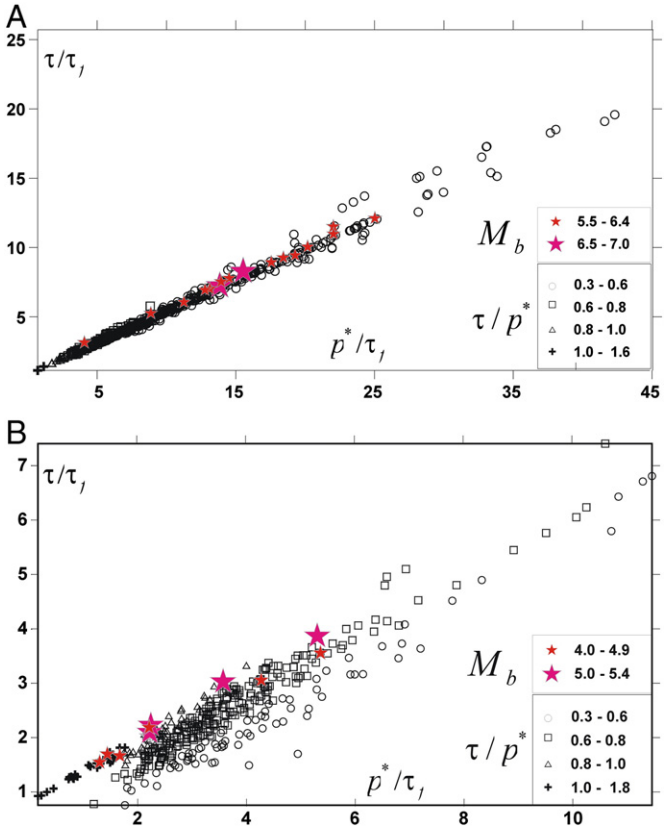

Fig. 16. Ratio of the reduced maximum shear stress τ/τ_f and the effective isotropic pressure p^*/τ_f for the crusts of Altai–Sayan (A) and Tien Shan (B). Asterisks correspond to the stress states of domains with strong earthquakes.

of large magnitudes are correlated with the zones of low level of effective pressure.

3.4. Analysis of regularity of distribution of stresses

Two main results of stress reconstruction in Altai–Sayan and Northern Tein Shan are: 1) correlation of orientation of principal stress axis and surface topography; 2) sharp changes of integral shear stresses acting on horizontal site in the crust when moving from Northern Tien Shan toward Altai–Sayan.

The analysis demonstrates that 75% of the domains in highlands axis of maximal compression of reconstructed stresses are sub-horizontal. Similarly, 75% of the domains in depressions axis of maximal compression of reconstructed stresses are sub-vertical. Because the highlands and inter-mountain depressions are neighbors, relationship between crust topography in orogens and acting tectonic regimes is shown in Fig. 15.

Sharp changes in the orientation of maximal compression from sub-horizontal in uplifted areas to sub-vertical in neighbor depressions are important factors for correcting the understanding of the current stress-state of the study regions. Another key-point of the problem can be the data on the orientation of underthrusting shear stresses. 90° change of orientation of these stresses obtained as reconstruction result is difficult to explain due to pushing forces generated by Indian plate.

Data on parameters of current stress-state enables to solve problems not only of geodynamics, but also of earthquake source physics. In particular, we found that strong earthquakes occur within crust domains where effective confining pressure is low. Earlier similar results were obtained for oceanic plate boundaries of seismoactive regions (Rebetsky, 2005b, 2007, 2009b).

Please cite this article as: Rebetsky, Yu.L., et al., Development of inversion methods on fault slip data, Tectonophysics (2012), http://dx.doi.org/10.1016/j.tecto.2012.09.027

Because yielding state of rocks is defined by Coulomb–Mohr relationship relating effective normal and shear stresses over the brittle fracture plane, the effective confining pressure is correlated with maximal shear stresses (Fig. 16). As it was already noted, relatively large earthquakes occurred in domains with low level of effective confining pressure and maximal shear stresses.

This result well agrees with rock specimen failure experiments in laboratories (Byerlee, 1978; et al.) which emphasize the role of friction in brittle failure. From the other hand, in the regions of low confining pressure deviatory stresses are also low, which do not correspond to modern seismological hypothesis on earthquake generation in the crust under high deviatory stresses (Reid, 1910).

But earlier J. Rice (1980) noted that the result of experiments on rock failure pointed as most favorable places for brittle failure domains of average deviatory stresses because these are also domains where confining pressure also gets average values.

4. Conclusion

As it is demonstrated in the paper, the MCA gives possibility to solve the problem of stress generation mechanism in the crust based on a new approach. The set of stress tensor parameters obtained within this method enables to determine not only orientation but also relationship between spherical and deviatory components. Such set of parameters of natural stress essentially enlarges analysis power of modern geodynamics.

Separate elements of the MCA were used in other methods of tectonophysic analysis of stresses. In this method they are integrated into a united algorithm, thanks to the background geomechanics. From this basis lying upon principles of plasticity theory, parameters of stress tensor are defined which ensure the best fit to the observed displacements in terms of energy, i.e. dissipation of energy through slip faults (Eq. (11)). This constraint modifies function (13), which has to be optimized. In the MCA, within this energetic principle mutually consistent parameters of stress ellipsoid and increment tensor of seismotectonic deformations (Eq. (9)) are calculated. This was absent in all previous methods. The energetic principles make it possible to formulate criteria of generating homogeneous sample sets of slip faults (Eq. (4)). They superimpose more strong physically justified restrictions on possible orientation of principal stress axis, than criteria (5) proposed in earlier works (Angelier and Mechler, 1977; Carey and Bruneier, 1974; Gushchenko and Kuznetsov, 1979).

Acknowledgments

Yu.L. Rebetsky remembers gratefully very important period of collaboration with J. Angelier, F. Bergerat and M. Brune in the late 1990s, when the basic concepts of the MCA were formulated. Common publications of J. Angelier gave me a fresh view on the problem on inversion of discontinuous dislocations. Many thanks to W. Mooney, R. Simpson and J. Hardebeck at the U.S. Geology Survey (the Menlo Park); co-operation with them drive me to upgrade the method. Special thanks to O.I. Gushchenko who introduced me into this interesting world of tectonophysic studies. We acknowledge our colleagues who gave us the data used in this study.

This research was partly supported by grants from International Center of Science and Engineering (Project no. 1536), as well as by grants from RFBR (Russian Foundation for Basis Research): 12-05-00234-a, 12-05-00550-a, 11-05-98594-r_east_a, 10-05-00126-a, and 11-05-00361-a.

References

Aleksandrowski, P., 1985. Graphical determination of principal stress directions for slicken side lineation populations: an attempt to modify Arthaud's method. Journal Structure Geology 7, 73–82.

Anderson, E.M., 1951. The dynamics of faulting and dyke formation with application to Britain. Oliver and Boyd, 2nd ed. Edinburgh, 206 pp.

Angelier, J., 1975a. Sur l'analyse des deplacements dus au jeu d'une population de failles. Exemple en Crete (Grece). Comptes Rendus de l' Academie des Sciences Paris D 280, 1657-1660.

Angelier, J., 1975b. Sur un apport de'informatique a L'analyse structurale; Exemple de la tectonique cassante. Revue de Géographie Physique et de Géologie Dynamique XVII (Fasc. 2), 137–146.

Angelier, J., 1975c. Sur l'analyse de mesures recueillies dans des sites failles: l'utilite d'une confrontation entre les methodes dynamiques et cinematiquues. Comptes Rendus de l' Academie des Sciences Paris D 281, 1805–1808.

Angelier, J., 1979. Determination of mean principal directions of stresses for a given fault population. Tectonophysics 56, T17–T26.

Angelier, J., 1989a. Inversion of filed data in fault tectonics to obtain the regional stress—II. Using conjugate fault sets witin heterogeneous families for computing palaeostress axes. Geophysical Journal 96, 139–149.

Angelier, J., 1989b. From orientation to magnitude in paleostress determinations using fault slip data. Journal Structure Geology 11 (No. ½), 37–49.

Angelier, J., 1990. Inversion field data in fault tectonics to obtain the regional stress—III. A new rapid direct inversion method by analytical means. Geophysical Journal Interior 10, 363–367.

Angelier, J., Mechler, P., 1977. Sur une methode graphique de recherche des contraintes principales egalement utilisable en tectonique et en seismologie: la methode des diedres droits. Bulletin de la Société Géologique de France XIX (No. 6), 1309–1318.

Angelier, J., Gustchenko, O.I., Rebetsky, Y.L., Sainto, A., Ilyin, A., Vassiliev, N., Malutin, S., 1994. Relationships between stress fields and deformation along a compressive strike–slip belt: Caucasus and Crimea (Russia and Ukraine). Comptes Rendus de l' Academie des Sciences Paris D 319 (II), 341–348.

Arefiev, S.S., Aptekman, Z.J., Bykova, V.V., Pogrebchenko, V.V., 2005. The geometry of the focal zone of the Altai earthquake of September 27, 2003. Geophysical researches 2, 16–26 (in Russian).

Armijo, R., Cisternas, A., 1978. Un problem inverse en mircotectonique cassante. Comptes Rendus de l' Academie des Sciences Paris D 287, 595–598.

Arthaud, F., 1969. Methode de determination graphique des directions de raccourcissement, d'allogement et intermediare d'une population de failles. Bulletin de la Société Géologique de France 7, 729–737.

Batdorf, S.B., Budiansky, B., 1954. The mathematical theory of plasticity based on the concept of sliding. Journal of Aplication Mechanics 21, 321.

Bergerat, F., 1987. Stress fields in the European platform at the time of Africa–Eurasia collision. Tectonics 6, 99–132.

Bott, M.H.P., 1959. The mechanics of oblique slip faulting. Geological Magazine 96, 109–117.

Brace, W.F., 1972. Laboratory studies of stick–slip and their application to earthquakes. Tectonophysics 14, 189–200.

Brune, J., 1968. Seismic moment, seismicity and rate slip along major fault zones. Journal Geophysical Researches 73 (No. 2), 777–784.

Buslov, M.M., Klerkx, J., Abdarakhmanov, K., Devaux, D., Batalev, V.Yu, Kuchai, O.A., Dehandschutter, B., Muraliev, A., 2003. Recent strike slip deformation of northern Tien Shan. In: Storti, F., Holdsworth, R.E., Salvini, F. (Eds.), Intraplate Strike–Slip Deformation Belts. : Special Publication, 210. Geological Society, London, pp. 53–64.

Byerlee, J.D., 1968. Brittle–ductile transition in rocks. Journal of Geophysical Research 73 (No. 14), 4741–4750.

Byerlee, J.D., 1978. Friction of rocks. Pure and Application Geophysics 116, 615–626.

Carey, E., Bruneier, B., 1974. Analyse theorique et numerique d'un modele mecanique elementaire applique a l'etude d'une populaton de failles. Comptes Rendus de l' Academie des Sciences Paris D 279, 891–894.

Chediya, O.K., 1986. Morphological Structure and the Latest Tectonic Tien Shan. USSR, Frunze, Ilim. 315 pp. (in Russian).

Chernykh, K.F., 1988. Introduction to Anisotropic Elasticity. Nauka, Moscow 190 pp. (in Russian).

Cobbold, P., Davy, P., 1988. Indentation tectonics in nature and experiment. 2. Central Asia. Bulletin of the Geological Institute University of Uppsala 144, 143–182.

Danilovich, V.N., 1961. A method of fault belts around big rupture in research discontinue displacements. Irkutsk. 47 pp. (in Russian).

Drucker, D.C., 1949. Relations of experiments to mathematical theories of plasticity. Journal of Applied Mechanics 16, 349–357.

England, P., Molnar, H., 1997. Active deformation of Asia: from kinematics to dynamics. Science 278 (5338), 647–650.

Etchecopar, A., Vasseur, G., Daignieres, M., 1981. An inverse problem in microtectonics for the determination of stress tensors from fault striation analysis. Journal Structure Geology 3, 51–65.

Gephart, J.W., 1985. Principal stress direction and the ambiguity in fault plane indification from focal mechanisms. Bulletin of the Seismological Society of America 75 (No. 2), 621–625.

Gephart, J.W., Forsyth, D.W., 1984. An improved method for determining the regional stress tensor using earthquake focal mechanism data: application to the San Fernando earthquake sequence. Journal Geophysical Researches 89 (No. B11), 9305–9320.

Gintov, O.B., Isai, V.M., 1984a. I. Some patterns of faulting and methods of analysis morfokinematic slip of faults. Geophysical Journal, 6 (No.3) 3–10 (in Russian).

Gintov, O.B., Isai, V.M., 1984b. II. Some patterns of faulting and methods of analysis morfokinematic slip of faults. Geophysical Journal, 6 (No. 4) 3–14 (in Russian).

Gushchenko, O.I., 1975. Kinematic principle of reconstruction of principal stress directions (on the geological and seismological data). Doklady Academian Science USSR. Series Geophysical 225 (No. 3), 557–560 (in Russian).

Please cite this article as: Rebetsky, Yu.L., et al., Development of inversion methods on fault slip data, Tectonophysics (2012), http://dx.doi.org/10.1016/j.tecto.2012.09.027

Gushchenko, O.I., 1979. The method of the kinematic analysis of structures of destruction at reconstruction of fields of tectonic stresses. Fields of Stress a Lithosphere. Nauka, Moscow, pp. 7–25 (in Russian).
Gushchenko, O.I., Kuznetsov, V.A., 1979. Determination of the orientations and the ratio of principal stresses on the basin of tectonic fault slip data. Stress Fields in the Lithosphere. Nauka, Moscow, pp. 60–66 (in Russian).
Gushchenko, O.I., Sim, L.A., 1974. Justification of the method of stress state reconstruction of the crust by orientation of the tectonic fault slip data (on the geological and seismological data). Mechanics of the Lithosphere, Sc.&Tech. Conf., 23–25 October 1974, Apatity-Moscow, pp. 5–8 (in Russian).
Gzovsky, M.V., 1954. Tectonic stress field. Izvestia Academian Science USSR. Series Geophysical 3, 390–410 (in Russian).
Gzovsky, M.V., 1956. Relation between tectonic faults and stresses in the Earth's crust. Exploration and Protection of Natural Resources, 11. Nauka, Moscow, pp. 7–22 (in Russian).
Handin, J., 1969. On the Colombo–Mohr failure criterion. Journal of Geophysical Research 74 (No. 22), 5343–5348.
Hill, R., 1950. Mathematical theory of plasticity. Oxford, 362 pp.
Kostrov, B.V., 1975. Mechanics of the Source of Tectonic Earthquake. Nauka Press, Moscow . 176 pp. (in Russia).
Kostrov, B.V., Das, Sh., 1988. Principles of Earthquake Source Mechanics. Camridge University Press, 174 pp.
Krestnikov, V.N., Belousov, T.P., Ermilin, V.I., Tchigarev, N.V., Shtrange, D.V., 1976. Quaternary Tectonics of the Pamir and Tien Shan. Nauka, Moscow, p. 116 (in Russian).
Lienert, B.R., Berg, E., Frazer, L.N., 1986. Hypocenter: An earthquake location method using centered, scaled, and adaptively damped least squares. Bulletin of the Seismological Society of America 76 (No. 3), 771–783.
Lisle, R., 1979. The representation and calculation of the deviatoric component of geological stress tensor. Journal Structure Geology 1, 317–321.
Lisle, R., 1987. Principal stress orientation from faults: an additional constrain. Annales Tectonicae 1, 155–158.
Lisle, R., 1992. New method of estimating regional stress orientation: application to focal mechanism data of recent British earthquakes. Geophysical Journal International 110, 276–282.
Makarov, V.I., 1977. The Latest Tectonic Structure of the Central Tien Shan. Nauka, Moscow. 172 pp. (in Russian).
McKenzie, D.P., 1969. The relation between fault plane solutions for earthquakes and directions of the principal stresses. Bulletin of the Seismological Society of America 59 (No. 2), 591–601.
Mercier, J., Vergely, P., Delibassis, N., 1973. Comparison entre les deformations deduites de l'analysise des failles recentes et des mecanismes au foyer des seismes (un exemple: la region de Paphos, Chypre). Tectonophysics 19, 315–332.
Michael, A.J., 1984. Determination of stress from slip data: faults and folds. Journal Geophysical Researches 89 (No. B11), 11517–11526.
Mogi, K., 1964. Deformation and fracture of rocks under confining pressure (2) compression test on dry rock sample. Bull. of the Earthquake Research Institute (Univ. Tokyo) 43 (Part 3), 491–514.
Mostrjukov, A.O., Petrov, V.A., 1994. The Catalogue of Mechanisms of the Centers of Earthquakes 1964–1990. Materials of the World Centre of the Data. Publishing house of the Russian Academy of Sciences, Moscow, p. 88 (in Russian).
Nadai, A., Wahl, A.M., 1931. Plasticity, a Mechanics of the Plastic State of Matter. New York, 349 pp.
Nikitin, L.V., Yunga, S.L., 1977. Methods of theoretical determination of tectonic deformation and stress in seismically active areas. Izvestia USSR. Physics of the Earth 11, 54–67 (in Russian).
Nikolaev, N.N., 1988. Contemporary Tectonics and Geodynamics of the Lithosphere. Nedra, Moscow. 492 pp. (in Russian).
Osokina, D.N., 1987. The relationship of the displacement discontinuities of tectonic stress fields and some of the issues of destruction massif. Fields of the Stress and Strain in the Crust. Nauka, Moscow, pp. 120–135 (in Russian).
Parfyonov, V.D., 1981. The stress analysis in anhydride tectonics. Doklady USSR 260 (No. 3), 695–698 (in Russian).
Reasenberg, P.A., Oppenheimer, D., 1985. FPFIT, FPPLOT and FPPAGE: Fortran computer programs for calculating and displaing earthquake fault-plane solutions. U.S. Geological Servey 345 Middlefield Road Menlo Park. California Open-File Report. No.85. 739.
Rebetsky, Yu.L., 1996. I. Stress-monitoring: issues of reconstruction methods of tectonic stresses and seismotectonic deformations. Journal of Earthquake Prediction Research 5 (No. 4), 557–573.
Rebetsky, Yu.L., 1997. Reconstruction of tectonic stresses and seismotectonic strain: methodical fundamentals, current stress field of Southeastern Asia and Oceania. Translation (Doklady) of the Russian Academy of Science 354 (No. 4), 560–563.
Rebetsky, Yu.L., 1998a. Recent stress field of Eastern Mediterranean on the base of seismological data about earthquake focal mechanisms. Annalees Geophysicae 16 (Part 1, Supl. 1), 49.
Rebetsky, Yu.L., 1998b. Methodical problems and techniques of reconstruction of tectonic stresses and seismotectonic deformations using the slip fault analysis. Annalees Geophysicae 16 (Part 1, Supl. 1), 28.
Rebetsky, Yu.L., 1999. Methods for reconstructing tectonic stresses and seismotectonic deformations based on the modern theory of plasticity. Doklady Earth Sciences 365A (No. 3), 370–373.
Rebetsky, Yu.L., 2003. Development of the method of cataclastic analysis of shear fractures for tectonic stress estimation. Doklady Earth Sciences 388 (No. 1), 72–76.
Rebetsky, Yu.L., 2005a. Evaluation of the relative values of the stress — the second stage of reconstruction according to the discontinuous displacements. Geophysical Journal 27 (No. 1), 39–54 (in Russian).
Rebetsky, Yu.L., 2005b. Tectonic stress, metamorphism, and earthquake source model. Doklady Earth Sciences 400 (No. 1), 127–131.
Rebetsky, Yu.L., 2007. Tectonic Stresses and the Strength of Rock. Nauka, Moscow. 406 pp. (in Russian).
Rebetsky, Yu.L., 2009a. The third and fourth stages of the reconstruction of the stresses in the method of cataclastic analysis of fault slip data. Geophysical Journal 31 (No. 2), 93–106 (in Russian).
Rebetsky, Yu.L., 2009b. Estimation of stress values in the method of cataclastic analysis of shear fracture. Doklady Earth Sciences 428 (No. 7), 1202–1207.
Rebetsky, Yu.L., 2009c. Stress state of the Earth's crust of the Kurils Islands and Kamchatka before the Simushir earthquake. Russian Journal Pacific Geology 3 (No. 5), 477–490.
Rebetsky, Yu.L, Fursova, E., 1997. Modern stress state of the South-East Asia and Oceania: Method of quasiplastic analysis. European Conference "Earth's Upper Mantle Structure Based on Integrated Geological and Geophysical Studies", Russia, Moscow, 17–19 April.
Rebetsky, Yu.L., Marinin, A.V., 2006a. Stress state of Earth's crust in the western region of Sunda subduction zone before the Sumatra–Andaman earthquake on December 26, 2004. Doklady Earth Sciences 407 (No. 2), 812–815.
Rebetsky, Yu.L., Marinin, A.V., 2006b. Preseismic stress field before Sumatra–Andaman earthquake of 26.12.2004. A model of metastable state of rocks. Geology and Geophysics 47 (No. 11), 1173–1185 (in Russian).
Rebetsky, Yu.L., Aref'ev, S.S., Nikitina, E.S., 2001. Monitoring of stressed state in the aftershock region of the Spitak earthquake. Doklady Earth Sciences 375 (No. 8), 1329–1333.
Reches, Z., 1978. Analysis of faulting in three-dimensional strain field. Tectonophysics 47, 109–129.
Reches, Z., 1983. Faulting of rock in three dimensional strain fields. II. Theoretical analysis. Tectonophysics 95, 133–156.
Reches, Z., 1987. Determination of the tectonic stress tensor from slip along faults that obey the Coulomb yield condition. Tectonics 6 (No. 6), 849–861.
Reid, H.F., 1910. The mechanism of the earthquake. The California earthquake of April 18, 1906. Rep. of the state investigation commiss. Washington. V. 2. pt. 1. 56 pp.
Rice, J., 1980. The Mechanics of Earthquake Rupture. North-Holland Publ.Comp., Amsterdam. 200 pp.
Rivera, L., Cirsternas, A., 1990. Stress tensor and fault plane solutions for a population of earthquakes. Bulletin of the Seismological Society of America 80 (No. 3), 600–614.
Riznichenko, Yu.V., 1965. On the seismic flow of rock masses. Dynamics of the Earth's crust. Nauka, USSR, Moscow, pp. 56–63 (in Russian).
Riznichenko, Yu.V., 1977. Estimation of strain rate in seismic flow of rocks. Izvestia. Academian Science USSR. Ser. Fizika Zemli 11, 34–47 (in Russian).
Roecker, S.W., Sabitova, T.M., Vinnik, L.P., Burmakov, Y.A., Golvanov, M.I., Mamatkanova, R., Munirova, L., 1993. Three-dimensional elastic wave velocity structure of the western and central Tien-Shan. Journal of Geophysical Research 98 (No. B9), 15779–15795.
Soboleva, O.V., Kuchay, O.A., Shklyar, G.P., Blagoveschenskaya, E.E., 1980. Catalog of earthquake focal mechanisms in Tajikistan and northern Afghanistan for the years 1959–1979. Moscow, VINITI. Deposited 2243. 25 pp. (in Russian).
Solonenko, A.V., Solonenko, N.A., Melnikova, V.I., Kozmin, B.M., Kuchay, O.A., Sukhanova, S.S., 1993. Stress and slip in the earthquakes foci of Siberia and Mongolia. Seismicity and Seismic Zoning of Northern Eurasia 1, Moscow, IPE RAS, pp. 113–122 (in Russian).
Stepanov, V.V., 1979. Quantifying tectonic strain. Fields of Stress and Strain in the Lithosphere. Nauka, Moscow, pp. 67–71 (in Russian).
Sychev, N.A., Aladjev, A.V., Mukhamadiev, V.A., Young, S.L., 2003. Study of focal mechanisms of foci according to the network KNET. Geodynamics and Geoecological Problems Highland regions, Moscow, pp. 241–253 (in Russian).
Sycheva, N.A., Bogomolov, L.M., Sychev, N.A., Kostuk, A.D., 2009. Intensity of seismotectonic strain as reference dynamic process in the Earth's crust. Russian conference "Tectonophysics and Problem of Earth's Science", Russia, Moscow, IFZ RAN, pp. 374–382.
Terzaghi, K., 1943. Theoretical Soil Mechanics. John Wiley and Sons, New York, 506 pp.
Trifonov, V.G., Soboleva, O.V., Trifonov, R.V., Vostrikov, G.A., 2002. Recent Geodynamics of the Alpine–Himalayan Collision Belt (in Russian). GEOS, Moscow. 224 pp.
Trifonov, V.U., Artushkov, E.V., Dodnov, A.E., Bachmankv, D.M., Mikolaichuk, A.V., Vishniakov, F.A., 2008. Pliocene–Quaternary mountain building in the central Tien Shan. Geology and Geophysics 49 (No. 2), 128–145 (in Russian).
Wallace, R.E., 1951. Geometry of shearing stress and relation to faulting. Journal of Geology (No. 59), 18–130.
Wells, D.L., Coppersmith, K.J., 1994. New empirical relationship among magnitude, rupture length, rupture width, rupture area, and surface displacement. Bulletin of the Seismological Society of America 84 (No. 4), 974–1002.
Yamaji, A., 2000. The multiple inverse method: a new technique to separate stresses from heterogeneous fault–slip data. Journal Structure Geology 22, 441–452.
Yunga, S.L., 1979. On the mechanism of deformation of seismically active crust Mathematics in USSR Ser. Physics of the Earth 6, 14–23 (in Russian).
Yunga, S.L., 1990. Methods and results of the study of seismotectonic strain. Nauka, Moscow. 190 pp. (in Russian).

Please cite this article as: Rebetsky, Yu.L., et al., Development of inversion methods on fault slip data, Tectonophysics (2012), http://dx.doi.org/10.1016/j.tecto.2012.09.027